

Forward-backward asymmetries of $\bar{B} \rightarrow \bar{K}_1(1270)\ell^+\ell^-$ and $\bar{B} \rightarrow \bar{K}^*\ell^+\ell^-$ transitions in two Higgs doublet model

F. Falahati* and A. Zahedidareshouri

Physics Department, Shiraz University, Shiraz 71454, Iran

(Received 28 July 2014; published 1 October 2014)

In this paper the polarized and unpolarized lepton pair forward-backward asymmetries and their averages in $\bar{B} \rightarrow \bar{K}_1(1270)\ell^+\ell^-$ and $\bar{B} \rightarrow \bar{K}^*\ell^+\ell^-$ decays using model III of the two Higgs doublet model are investigated. The obtained results of both decay modes are compared to each other and to those of SM. In addition, by obtaining the minimum required number of events for detecting each asymmetry and comparing them with the number of produced $B\bar{B}$ pairs at the LHC or supposed to be produced at the Super-LHC, we present a comprehensive discussion regarding the polarized and unpolarized forward-backward asymmetries of $\bar{B} \rightarrow \bar{K}_1(1270)\ell^+\ell^-$ and $\bar{B} \rightarrow \bar{K}^*\ell^+\ell^-$ decays. We discover that the study of these asymmetries and the corresponding averages in $\bar{B} \rightarrow \bar{K}_1(1270)\ell^+\ell^-$ and $\bar{B} \rightarrow \bar{K}^*\ell^+\ell^-$ decays can provide good signals for probing new physics beyond the SM in the future B-physics experiments.

DOI: [10.1103/PhysRevD.90.075002](https://doi.org/10.1103/PhysRevD.90.075002)

PACS numbers: 12.60.-i, 13.30.-a, 14.20.Mr

I. INTRODUCTION

The flavor-changing neutral currents (FCNC) $b \rightarrow s\ell^+\ell^-$ ($\ell = e, \mu, \tau$), forbidden in the standard model (SM) at the tree level, are very sensitive to the flavor structure of the SM and to the new physics (NP) beyond the SM. Lately, the rare decays $\bar{B} \rightarrow \bar{K}_1\ell^+\ell^-$ involving axial-vector strange mesons have been the matter of many theoretical discussions either in the framework of the SM [1–4] or in the framework of some new physics models, such as models including a universal extra dimension [5], supersymmetry particles [6], the fourth-generation fermions [7], and the nonuniversal Z' model [8]. Generally, by studying these semileptonic decays, a number of physical observables such as branching ratio, the forward-backward asymmetry, and lepton polarization asymmetry, which have important roles in testing SM and in probing possible NP models, could be investigated.

In the quark model, the two lowest nonets of $J^P = 1^+$ axial-vector mesons are usually the orbitally excited $q\bar{q}'$ states. In the context of the spectroscopic notation, these nonets correspond to two types of lowest p -wave mesons, specifically, 1^3P_1 and 1^1P_1 . The two nonets have distinctive C quantum numbers, $C = +$ or $C = -$, respectively. Experimentally, while the $J^{PC} = 1^{++}$ nonet contains $a_1(1260)$, $f_1(1285)$, $f_1(1420)$, and K_{1A} , the 1^{+-} nonet consists of $b_1(1235)$, $h_1(1170)$, $h_1(1380)$, and K_{1B} . The physical states $K_1(1270)$ and $K_1(1400)$ are the mixtures of 1^3P_1 (K_{1A}) and 1^1P_1 (K_{1B}) states. K_{1A} and K_{1B} are not mass eigenstates and they can be mixed together due to the strange and nonstrange light quark mass difference. Considering the convention given in Ref. [1], their relations can be written as

$$\begin{pmatrix} |\bar{K}_1(1270)\rangle \\ |\bar{K}_1(1400)\rangle \end{pmatrix} = M \begin{pmatrix} |\bar{K}_{1A}\rangle \\ |\bar{K}_{1B}\rangle \end{pmatrix},$$

with $M = \begin{pmatrix} \sin\theta & \cos\theta \\ \cos\theta & -\sin\theta \end{pmatrix}$. (1)

The SM of electroweak interactions has been strictly tested over the past 20 years and shows an excellent compatibility with all collider data. The dynamics of electroweak symmetry breaking, however, is not exactly known. While the simplest possibility is the minimal Higgs mechanism which suggests a single scalar SU(2) doublet, many extensions of the SM predict a large Higgs sector to contain more scalars [9,10].

Two conditions which tightly constrain the extensions of the SM Higgs sector are first the value of the rho parameter, $\rho \equiv M_W^2/M_Z^2\cos^2\theta_w \simeq 1$, where M_W (M_Z) is the W^\pm (Z) boson mass and θ_w is the weak mixing angle; and second the absence of large flavor-changing neutral currents. The first of these conditions is spontaneously fulfilled by Higgs sectors that consist only of SU(2) doublets (with the possibly additional singlets). The simplest such model that contains a charged Higgs boson is a two Higgs doublet model (2HDM). The second of these conditions is spontaneously satisfied by models in which the masses of fermions are produced through couplings to exactly one Higgs doublet; this is known as natural flavor conservation and forbids the tree-level flavor-changing neutral Higgs interactions phenomena.

If we impose natural flavor conservation by considering an *ad hoc* discrete symmetry [11], there would be two different ways to couple the SM fermions to two Higgs doublets. The type-I and type-II 2HDMs, which have been studied extensively in the literature, are such models [10]. Without considering discrete symmetry, a more general

*falahati@shirazu.ac.ir

form of 2HDM, namely, model III, has been obtained which allows for the presence of FCNC at tree level. Consistent with the low energy constraints, the FCNC involving the first two generations are highly suppressed, and those involving the third generation are not as severely suppressed as the first two generations. Also, in such a model there exists rich induced CP -violating sources from a single CP phase of vacuum that is absent in the SM, model I and model II. In order to consider the flavor-conserving limit of type III, we suppose that the two Yukawa matrices for each fermion type are diagonal in the same fermion mixing basis [12]. All three structures of 2HDM generally contain two scalar Higgs bosons h^0, H^0 , one pseudoscalar Higgs boson A^0 , and one charged Higgs boson H^\pm .

Motivated by the above paragraphs, we shall address the effects of model III of 2HDM in the rare decays $\bar{B} \rightarrow \bar{K}_1(1270)\ell^+\ell^-$. Also, we consider the influences of such model on the $\bar{B} \rightarrow \bar{K}^*\ell^+\ell^-$ decays. In such a way, we present a comprehensive analysis for the polarized and unpolarized forward-backward asymmetries of $\bar{B} \rightarrow \bar{K}_1(1270)\ell^+\ell^-$ and $\bar{B} \rightarrow \bar{K}^*\ell^+\ell^-$ decays and study the sensitivity of results to the vector property or the axial-vector property of produced mesons.

The remainder of this paper is organized as follows. In Sec. II, we first present the expressions for the matrix elements of B to an axial-vector meson and B to a vector meson, here $\bar{B} \rightarrow \bar{K}_1(1270)\ell^+\ell^-$ and $\bar{B} \rightarrow \bar{K}^*\ell^+\ell^-$,

respectively, in SM and 2HDM. Then the general expressions for the polarized and unpolarized lepton pair forward-backward asymmetries have been extracted out. The sensitivity of these polarizations and the corresponding averages to the model III 2HDM parameters have been numerically analyzed in Sec. III. In the final section, a summary of concluding remarks is presented.

II. ANALYTIC FORMULAS

A. The effective Hamiltonian for $\bar{B} \rightarrow \bar{K}^*\ell^+\ell^-$ and $\bar{B} \rightarrow \bar{K}_1\ell^+\ell^-$ transitions in SM and 2HDM

By integrating out the heavy degrees of freedom containing top quark, W^\pm and Z bosons above scale $\mu = O(m_b)$, the governing effective Hamiltonian for $\bar{B} \rightarrow \bar{K}^*\ell^+\ell^-$ and $\bar{B} \rightarrow \bar{K}_1\ell^+\ell^-$ transitions, described by $b \rightarrow s\ell^+\ell^-$, in SM is represented as [13,14]

$$\mathcal{H}_{\text{eff}}(b \rightarrow s\ell^+\ell^-) = -\frac{G_F}{2\sqrt{2}} V_{tb} V_{ts}^* \sum_{i=1}^{10} C_i(\mu) O_i(\mu), \quad (2)$$

where we have omitted the terms proportional to $V_{ub} V_{us}^*$ because of $|V_{ub} V_{us}^* / V_{tb} V_{ts}^*| < 0.02$. The local operators are introduced in [13,14]. Also, considering the same division in 2HDM, the effective Hamiltonian of the above-mentioned decays could be obtained as [15]

$$\mathcal{H}_{\text{eff}}(b \rightarrow s\ell^+\ell^-) = -\frac{4G_F}{\sqrt{2}} V_{tb} V_{ts}^* \left\{ \sum_{i=1}^{10} C_i(\mu) O_i(\mu) + \sum_{i=1}^{10} C_{Q_i}(\mu) Q_i(\mu) \right\}, \quad (3)$$

where the first part is related to the effective Hamiltonian in the SM such that the respective Wilson coefficients get additional contributions because of charged Higgs diagrams. The second part involving new operators originates from integrating out the effects of massive neutral Higgs bosons; these new operators as well as the corresponding Wilson coefficients are given in [13,15]. Now, using the aforementioned effective Hamiltonian in 2HDM, the one-loop matrix elements of $b \rightarrow s\ell^+\ell^-$ can be given as

$$\begin{aligned} \mathcal{M} &= \langle s\ell^+\ell^- | \mathcal{H}_{\text{eff}} | b \rangle \\ &= -\frac{G_F \alpha}{2\sqrt{2}\pi} V_{tb} V_{ts}^* \left\{ \tilde{C}_9^{\text{eff}} \bar{s} \gamma_\mu (1 - \gamma_5) b \bar{\ell} \gamma^\mu \ell + \tilde{C}_{10} \bar{s} \gamma_\mu (1 - \gamma_5) b \bar{\ell} \gamma^\mu \gamma_5 \ell \right. \\ &\quad - 2C_7^{\text{eff}} \frac{m_b}{q^2} \bar{s} i \sigma_{\mu\nu} q^\nu (1 + \gamma_5) b \bar{\ell} \gamma^\mu \ell - 2C_7^{\text{eff}} \frac{m_s}{q^2} \bar{s} i \sigma_{\mu\nu} q^\nu (1 - \gamma_5) b \bar{\ell} \gamma^\mu \ell \\ &\quad \left. + C_{Q_1} \bar{s} (1 + \gamma_5) b \bar{\ell} \ell + C_{Q_2} \bar{s} (1 + \gamma_5) b \bar{\ell} \gamma_5 \ell \right\}, \quad (4) \end{aligned}$$

where the Wilson coefficients C_7^{eff} , \tilde{C}_9^{eff} , \tilde{C}_{10} , C_{Q_1} , and C_{Q_2} are calculated at the scale m_b . For obtaining the effective coefficients C_7^{eff} , \tilde{C}_9^{eff} , and \tilde{C}_{10} at the scale m_b , the values of coefficients C_7 , \tilde{C}_9 , and \tilde{C}_{10} at the scale m_W are needed. These coefficients which get additional terms compared to those of in SM, by adding the contributions due to the charged Higgs bosons' exchange diagrams, are given in [13,15]. Also, the evolution of coefficients C_{Q_1} and C_{Q_2} are taken into account in [15].

It should be noted that the coefficient $\tilde{C}_9^{\text{eff}}(\mu, q^2) \equiv \tilde{C}_9(\mu) + Y(\mu, q^2)$, where the function Y contains the short distance contributions from the one-loop matrix elements of the four-quark operators, $Y_{\text{per}}(q^2)$, as well as the long distance effects

associated with real $c\bar{c}$ in the intermediate states, $Y_{\text{LD}}(q^2)$. Therefore, $Y(q^2) = Y_{\text{per}}(q^2) + Y_{\text{LD}}(q^2)$. The function $Y_{\text{per}}(q^2)$ is given by

$$\begin{aligned} Y_{\text{per}}(q^2) &= g\left(\frac{m_c}{m_b}, s\right)(3C_1 + C_2 + 3C_3 + C_4 + 3C_5 + C_6) \\ &\quad - \frac{1}{2}g(1, s)(4C_3 + 4C_4 + 3C_5 + C_6) \\ &\quad - \frac{1}{2}g(0, s)(C_3 + 3C_4) + \frac{2}{9}(3C_3 + C_4 + 3C_5 + C_6), \end{aligned} \quad (5)$$

where the explicit expressions for the g functions can be found in [13]. On the contrary, the long-distance contributions $Y_{\text{LD}}(z, \hat{s})$ cannot be calculated and are usually parametrized in the form of a phenomenological Breit-Wigner formula:

$$Y_{\text{LD}} = \frac{3\pi}{\alpha^2} C^{(0)} \sum_{V_i=\psi, \psi', \dots} k_i \frac{\Gamma(V_i \rightarrow \ell^+ \ell^-) m_{V_i}}{m_{V_i}^2 - q^2 - im_{V_i} \Gamma_{V_i}},$$

where α is the fine structure constant and $C^{(0)} = (3C_1 + C_2 + 3C_3 + C_4 + 3C_5 + C_6)$. The phenomenological parameters k_i for the $\bar{B} \rightarrow \bar{K}^* \ell^+ \ell^-$ decay can be fixed from $\text{Br}(\bar{B} \rightarrow J/\psi \bar{K}^* \rightarrow \bar{K}^* \ell^+ \ell^-) = \text{Br}(\bar{B} \rightarrow J/\psi \bar{K}^*) \text{Br}(J/\psi \rightarrow \ell^+ \ell^-)$. For the lowest resonances ψ and ψ' we will use $k = 1.65$ and $k = 2.36$, respectively [16]. Also, for the $\bar{B} \rightarrow \bar{K}_1 \ell^+ \ell^-$ decay such parameters can be determined by $\text{Br}(\bar{B} \rightarrow J/\psi \bar{K}_1 \rightarrow \bar{K}_1 \ell^+ \ell^-) = \text{Br}(\bar{B} \rightarrow J/\psi \bar{K}_1) \text{Br}(J/\psi \rightarrow \ell^+ \ell^-)$. However, since the

branching ratio of $\bar{B} \rightarrow J/\psi \bar{K}_1$ decay has not been measured yet, we assume that the values of k_i are of the order of 1. Therefore, we use $k_1 = 1$ and $k_2 = 1$ in the following numerical calculations.

B. Form factors for $\bar{B} \rightarrow \bar{K}^* \ell^+ \ell^-$ transition

The exclusive $\bar{B} \rightarrow \bar{K}^* \ell^+ \ell^-$ decay is described in terms of the matrix elements of the quark operators in Eq. (4) over meson states, which can be parametrized in terms of the form factors. Obviously, the following matrix elements,

$$\begin{aligned} &\langle \bar{K}^* | \bar{s} \gamma_\mu (1 - \gamma_5) b | \bar{B} \rangle, \\ &\langle \bar{K}^* | \bar{s} i \sigma_{\mu\nu} q^\nu (1 \pm \gamma_5) b | \bar{B} \rangle, \\ &\langle \bar{K}^* | \bar{s} (1 + \gamma_5) b | \bar{B} \rangle, \end{aligned} \quad (6)$$

are needed for the calculation of the $\bar{B} \rightarrow \bar{K}^* \ell^+ \ell^-$ decay. These matrix elements are defined as follows:

$$\begin{aligned} \langle \bar{K}^*(p_{K^*}, \lambda) | \bar{s} \gamma_\mu (1 \pm \gamma_5) b | \bar{B}(p_B) \rangle &= -\varepsilon_{\mu\nu\lambda\sigma} \varepsilon_{(\lambda)}^{*\nu} p_{K^*}^\lambda q^\sigma \frac{2V^{K^*}(q^2)}{m_B + m_{K^*}} \pm i\varepsilon_{\mu}^{(\lambda)*} (m_B + m_{K^*}) A_1^{K^*}(q^2) \\ &\mp i(p_B + p_{K^*})_\mu (\varepsilon_{(\lambda)}^* \cdot q) \frac{A_2^{K^*}(q^2)}{m_B + m_{K^*}} \mp iq_\mu \frac{2m_{K^*}}{q^2} (\varepsilon_{(\lambda)}^* \cdot q) [A_3^{K^*}(q^2) - A_0^{K^*}(q^2)], \end{aligned} \quad (7)$$

$$\begin{aligned} \langle \bar{K}^*(p_{K^*}, \lambda) | \bar{s} i \sigma_{\mu\nu} q^\nu (1 \pm \gamma_5) b | \bar{B}(p_B) \rangle &= 2\varepsilon_{\mu\nu\lambda\sigma} \varepsilon_{(\lambda)}^{*\nu} p_{K^*}^\lambda q^\sigma T_1^{K^*}(q^2) \pm i\varepsilon_{\mu}^{(\lambda)*} (m_B^2 - m_{K^*}^2) - (p_B + p_{K^*})_\mu (\varepsilon_{(\lambda)}^* \cdot q) T_2^{K^*}(q^2) \\ &\pm i(\varepsilon_{(\lambda)}^* \cdot q) \left[q_\mu - (p_B + p_{K^*})_\mu \frac{q^2}{m_B^2 - m_{K^*}^2} \right] T_3^{K^*}(q^2), \end{aligned} \quad (8)$$

where $q = p_B - p_{K^*}$ is the momentum transfer and ε is the polarization vector of the \bar{K}^* meson. Also, we assume that $A_3^{K^*}(q^2 = 0) = A_0^{K^*}(q^2 = 0)$ and $T_1^{K^*}(q^2 = 0) = T_2^{K^*}(q^2 = 0)$. Now, contracting both sides of Eq. (7) with q^μ and using the equation of motion, the matrix element $\langle \bar{K}^* | \bar{s} (1 \pm \gamma_5) b | \bar{B} \rangle$ is calculated as

$$\langle \bar{K}^*(p_{K^*}, \lambda) | \bar{s} (1 \pm \gamma_5) b | \bar{B}(p_B) \rangle = \pm \langle \bar{K}^*(p_{K^*}, \lambda) | \bar{s} \gamma_5 b | \bar{B}(p_B) \rangle = \frac{1}{m_b + m_s} [\mp 2im_{K^*} (\varepsilon_{(\lambda)}^* \cdot q) A_0^{K^*}(q^2)], \quad (9)$$

$$\langle \bar{K}^*(p_{K^*}, \lambda) | \bar{s} b | \bar{B}(p_B) \rangle = 0. \quad (10)$$

In deriving Eq. (9) we have used the relationship

$$2m_{K^*}A_3^{K^*}(q^2) = (m_B + m_{K^*})A_1^{K^*}(q^2) - (m_B - m_{K^*})A_2^{K^*}(q^2),$$

which follows from the equations of motion. For the form factors we have used the light cone QCD sum rules results [17] in which the q^2 dependence of the form factors is represented by

$$F(q^2) = \frac{F(0)}{1 - a_F(q^2/m_B^2) + b_F(q^2/m_B^2)^2}. \quad (11)$$

The values of parameters $F(0)$, a_F , and b_F for the $\bar{B} \rightarrow \bar{K}^* \ell^+ \ell^-$ decay are listed in Table I.

TABLE I. B meson decay form factors in a three-parameter fit, where the radiative corrections to the leading twist contribution and SU(3) breaking effects are taken into account.

F	$F(0)$	a_F	b_F
$A_1^{B \rightarrow K^*}$	0.34 ± 0.05	0.60	-0.023
$A_2^{B \rightarrow K^*}$	0.28 ± 0.04	1.18	0.281
$A_0^{B \rightarrow K^*}$	0.47 ± 0.07	1.55	0.680
$V^{B \rightarrow K^*}$	0.46 ± 0.07	1.55	0.575
$T_1^{B \rightarrow K^*}$	0.38 ± 0.06	1.59	0.615
$T_2^{B \rightarrow K^*}$	0.38 ± 0.06	0.49	-0.241
$T_3^{B \rightarrow K^*}$	0.26 ± 0.04	1.20	0.098

C. Form factors for $\bar{B} \rightarrow \bar{K}_1 \ell^+ \ell^-$ transition

Similar to the exclusive $\bar{B} \rightarrow \bar{K}^* \ell^+ \ell^-$ decay, the $\bar{B} \rightarrow \bar{K}_1 \ell^+ \ell^-$ transition is explained by the expressions that appear in Eq. (6), except K^* is replaced by K_1 . These matrix elements could be parametrized as

$$\begin{aligned} \langle \bar{K}_1(p_{K_1}, \lambda) | \bar{s} \gamma_\mu (1 \pm \gamma_5) b | \bar{B}(p_B) \rangle &= \pm i \frac{2}{m_B + m_{K_1}} \epsilon_{\mu\nu\rho\sigma} \epsilon_{(\lambda)}^* p_B^\rho p_{K_1}^\sigma A^{K_1}(q^2) + 2m_{K_1} \frac{\epsilon_{(\lambda)}^* \cdot p_B}{q^2} q_\mu [V_3^{K_1}(q^2) - V_0^{K_1}(q^2)] \\ &\quad - \left[(m_B + m_{K_1}) \epsilon_\mu^{(\lambda)*} V_1^{K_1}(q^2) - (p_B + p_{K_1})_\mu (\epsilon_{(\lambda)}^* \cdot p_B) \frac{V_2^{K_1}(q^2)}{m_B + m_{K_1}} \right], \end{aligned} \quad (12)$$

$$\begin{aligned} \langle \bar{K}_1(p_{K_1}, \lambda) | \bar{s} \sigma_{\mu\nu} q^\nu (1 \pm \gamma_5) b | \bar{B}(p_B) \rangle &= \pm 2T_1^{K_1}(q^2) \epsilon_{\mu\nu\rho\sigma} \epsilon_{(\lambda)}^* p_B^\rho p_{K_1}^\sigma - iT_3^{K_1}(q^2) (\epsilon_{(\lambda)}^* \cdot q) \left[q_\mu - \frac{q^2}{m_B^2 - m_{K_1}^2} (p_{K_1} + p_B)_\mu \right] \\ &\quad - iT_2^{K_1}(q^2) [(m_B^2 - m_{K_1}^2) \epsilon_\mu^{(\lambda)*} - (\epsilon_{(\lambda)}^* \cdot q) (p_B + p_{K_1})_\mu], \end{aligned} \quad (13)$$

$$\langle \bar{K}_1(p_{K_1}, \lambda) | \bar{s} (1 \pm \gamma_5) b | \bar{B}(p_B) \rangle = \langle \bar{K}_1(p_{K_1}, \lambda) | \bar{s} b | \bar{B}(p_B) \rangle = \frac{1}{m_b - m_s} [-2m_{K_1} (\epsilon_{(\lambda)}^* \cdot q) V_0^{K_1}(q^2)], \quad (14)$$

$$\langle \bar{K}_1(p_{K_1}, \lambda) | \bar{s} \gamma_5 b | \bar{B}(p_B) \rangle = 0, \quad (15)$$

with $q \equiv p_B - p_{K_1}$, $\gamma_5 \equiv i\gamma^0\gamma^1\gamma^2\gamma^3$, and $\epsilon^{0123} = -1$. Considering the equation of motion, the form factors satisfy the following relations:

$$\begin{aligned} V_3^{K_1}(0) &= V_0^{K_1}(0), \quad T_1^{K_1}(0) = T_2^{K_1}(0), \\ V_3^{K_1}(q^2) &= \frac{m_B + m_{K_1}}{2m_{K_1}} V_1^{K_1}(q^2) - \frac{m_B - m_{K_1}}{2m_{K_1}} V_2^{K_1}(q^2). \end{aligned} \quad (16)$$

Because the $\bar{K}_1(1270)$ and $\bar{K}_1(1400)$ are the mixing states of the \bar{K}_{1A} and \bar{K}_{1B} , the $\bar{B} \rightarrow \bar{K}_1$ form factors can be parametrized as

$$\begin{pmatrix} \langle \bar{K}_1(1270) | \bar{s} \gamma_\mu (1 \pm \gamma_5) b | \bar{B} \rangle \\ \langle \bar{K}_1(1400) | \bar{s} \gamma_\mu (1 \pm \gamma_5) b | \bar{B} \rangle \end{pmatrix} = M \begin{pmatrix} \langle \bar{K}_{1A} | \bar{s} \gamma_\mu (1 \pm \gamma_5) b | \bar{B} \rangle \\ \langle \bar{K}_{1B} | \bar{s} \gamma_\mu (1 \pm \gamma_5) b | \bar{B} \rangle \end{pmatrix}, \quad (17)$$

$$\begin{pmatrix} \langle \bar{K}_1(1270) | \bar{s} \sigma_{\mu\nu} q^\nu (1 \pm \gamma_5) b | \bar{B} \rangle \\ \langle \bar{K}_1(1400) | \bar{s} \sigma_{\mu\nu} q^\nu (1 \pm \gamma_5) b | \bar{B} \rangle \end{pmatrix} = M \begin{pmatrix} \langle \bar{K}_{1A} | \bar{s} \sigma_{\mu\nu} q^\nu (1 \pm \gamma_5) b | \bar{B} \rangle \\ \langle \bar{K}_{1B} | \bar{s} \sigma_{\mu\nu} q^\nu (1 \pm \gamma_5) b | \bar{B} \rangle \end{pmatrix}, \quad (18)$$

with the mixing matrix M being given in Eq. (1). Then the form factors A^{K_1} , $V_{0,1,2}^{K_1}$, and $T_{1,2,3}^{K_1}$ satisfy the following expressions:

$$\begin{pmatrix} A^{K_1(1270)}/(m_B + m_{K_1(1270)}) \\ A^{K_1(1400)}/(m_B + m_{K_1(1400)}) \end{pmatrix} = M \begin{pmatrix} A^{K_{1A}}/(m_B + m_{K_{1A}}) \\ A^{K_{1B}}/(m_B + m_{K_{1B}}) \end{pmatrix}, \quad (19)$$

$$\begin{pmatrix} (m_B + m_{K_1(1270)})V_1^{K_1(1270)} \\ (m_B + m_{K_1(1400)})V_1^{K_1(1400)} \end{pmatrix} = M \begin{pmatrix} (m_B + m_{K_{1A}})V_1^{K_{1A}} \\ (m_B + m_{K_{1B}})V_1^{K_{1B}} \end{pmatrix}, \quad (20)$$

$$\begin{pmatrix} V_2^{K_1(1270)}/(m_B + m_{K_1(1270)}) \\ V_2^{K_1(1400)}/(m_B + m_{K_1(1400)}) \end{pmatrix} = M \begin{pmatrix} V_2^{K_{1A}}/(m_B + m_{K_{1A}}) \\ V_2^{K_{1B}}/(m_B + m_{K_{1B}}) \end{pmatrix}, \quad (21)$$

$$\begin{pmatrix} m_{K_1(1270)}V_0^{K_1(1270)} \\ m_{K_1(1400)}V_0^{K_1(1400)} \end{pmatrix} = M \begin{pmatrix} m_{K_{1A}}V_0^{K_{1A}} \\ m_{K_{1B}}V_0^{K_{1B}} \end{pmatrix}, \quad (22)$$

$$\begin{pmatrix} T_1^{K_1(1270)} \\ T_1^{K_1(1400)} \end{pmatrix} = M \begin{pmatrix} T_1^{K_{1A}} \\ T_1^{K_{1B}} \end{pmatrix}, \quad (23)$$

$$\begin{pmatrix} (m_B^2 - m_{K_1(1270)}^2)T_2^{K_1(1270)} \\ (m_B^2 - m_{K_1(1400)}^2)T_2^{K_1(1400)} \end{pmatrix} = M \begin{pmatrix} (m_B^2 - m_{K_{1A}}^2)T_2^{K_{1A}} \\ (m_B^2 - m_{K_{1B}}^2)T_2^{K_{1B}} \end{pmatrix}, \quad (24)$$

$$\begin{pmatrix} T_3^{K_1(1270)} \\ T_3^{K_1(1400)} \end{pmatrix} = M \begin{pmatrix} T_3^{K_{1A}} \\ T_3^{K_{1B}} \end{pmatrix}, \quad (25)$$

where we have assumed $p_{K_1(1270),K_1(1400)}^\mu \simeq p_{K_{1A}}^\mu \simeq p_{K_{1B}}^\mu$ [1] for simplicity. For the form factors, we will use results calculated with light cone sum rules (LCSRs) [18], which are exhibited in Table II. In the whole kinematical region, the dependence of each form factor on momentum transfer q^2 is parametrized in the double-pole form:

$$F(q^2) = \frac{F(0)}{1 - a_F(q^2/m_B^2) + b_F(q^2/m_B^2)^2}. \quad (26)$$

And the nonperturbative parameters a_F and b_F can be fitted by the magnitudes of form factors corresponding to the small momentum transfer calculated in the LCSRs approach.

D. Formulas of observables for $\bar{B} \rightarrow \bar{K}_1 \ell^+ \ell^-$

Using Eq. (4) and the definitions of form factors, the decay amplitude for $\bar{B} \rightarrow \bar{K}_1 \ell^+ \ell^-$ can be written as follows:

$$\mathcal{M} = \frac{G_F \alpha_{\text{em}}}{2\sqrt{2}\pi} V_{ts}^* V_{tb} m_B \cdot (-i) \{ \mathcal{T}_\mu^{(K_1),1} \bar{\ell} \gamma^\mu \ell + \mathcal{T}_\mu^{(K_1),2} \bar{\ell} \gamma^\mu \gamma_5 \ell + \mathcal{T}^{(K_1),3} \bar{\ell} \ell + \mathcal{T}^{(K_1),4} \bar{\ell} \gamma_5 \ell \}, \quad (27)$$

where

$$\begin{aligned} \mathcal{T}_\mu^{(K_1),1} &= \mathcal{A}^{K_1}(\hat{s}) \varepsilon_{\mu\nu\rho\sigma} \varepsilon^{*\nu} \hat{p}_B^\rho \hat{p}_{K_1}^\sigma - i\mathcal{B}^{K_1}(\hat{s}) \varepsilon_\mu^* \\ &\quad + i\mathcal{C}^{K_1}(\hat{s}) (\varepsilon^* \cdot \hat{p}_B) \hat{p}_\mu + i\mathcal{D}^{K_1}(\hat{s}) (\varepsilon^* \cdot \hat{p}_B) \hat{q}_\mu, \end{aligned} \quad (28)$$

$$\begin{aligned} \mathcal{T}_\mu^{(K_1),2} &= \mathcal{E}^{K_1}(\hat{s}) \varepsilon_{\mu\nu\rho\sigma} \varepsilon^{*\nu} \hat{p}_B^\rho \hat{p}_{K_1}^\sigma - i\mathcal{F}^{K_1}(\hat{s}) \varepsilon_\mu^* \\ &\quad + i\mathcal{G}^{K_1}(\hat{s}) (\varepsilon^* \cdot \hat{p}_B) \hat{p}_\mu + i\mathcal{H}^{K_1}(\hat{s}) (\varepsilon^* \cdot \hat{p}_B) \hat{q}_\mu, \end{aligned} \quad (29)$$

$$\mathcal{T}^{(K_1),3} = i\mathcal{I}_1^{K_1}(\hat{s}) \frac{(\varepsilon^{(\lambda)*} \cdot \hat{q})}{1 + \hat{m}_s} + i\mathcal{J}_1^{K_1}(\hat{s}) \frac{(\varepsilon^{(\lambda)*} \cdot \hat{p}_B)}{1 + \hat{m}_s} \quad (30)$$

$$\mathcal{T}^{(K_1),4} = i\mathcal{I}_2^{K_1}(\hat{s}) \frac{(\varepsilon^{(\lambda)*} \cdot \hat{q})}{1 + \hat{m}_s} + i\mathcal{J}_2^{K_1}(\hat{s}) \frac{(\varepsilon^{(\lambda)*} \cdot \hat{p}_B)}{1 + \hat{m}_s}, \quad (31)$$

with $\hat{s} = q^2/m_B^2$, $\hat{p} = p/m_B$, $\hat{p}_B = p_B/m_B$, $\hat{q} = q/m_B$, $\hat{m}_s = m_s/m_B$, $\hat{m}_\ell = m_\ell/m_B$, and $p = p_B + p_{K_1}$,

TABLE II. Form factors for $B \rightarrow K_{1A}, K_{1B}$ transitions obtained in the LCQSR calculation are fitted to the three-parameter form (26).

F	$F(0)$	a	b	F	$F(0)$	a	b
$V_1^{BK_{1A}}$	0.34 ± 0.07	0.635	0.211	$V_1^{BK_{1B}}$	$-0.29^{+0.08}_{-0.05}$	0.729	0.074
$V_2^{BK_{1A}}$	0.41 ± 0.08	1.51	1.18	$V_2^{BK_{1B}}$	$-0.17^{+0.05}_{-0.03}$	0.919	0.855
$V_0^{BK_{1A}}$	0.22 ± 0.04	2.40	1.78	$V_0^{BK_{1B}}$	$-0.45^{+0.12}_{-0.08}$	1.34	0.690
$A^{BK_{1A}}$	0.45 ± 0.09	1.60	0.974	$A^{BK_{1B}}$	$-0.37^{+0.10}_{-0.06}$	1.72	0.912
$T_1^{BK_{1A}}$	$0.31^{+0.09}_{-0.05}$	2.01	1.50	$T_1^{BK_{1B}}$	$-0.25^{+0.06}_{-0.07}$	1.59	0.790
$T_2^{BK_{1A}}$	$0.31^{+0.09}_{-0.05}$	0.629	0.387	$T_2^{BK_{1B}}$	$-0.25^{+0.06}_{-0.07}$	0.378	-0.755
$T_3^{BK_{1A}}$	$0.28^{+0.08}_{-0.05}$	1.36	0.720	$T_3^{BK_{1B}}$	-0.11 ± 0.02	-1.61	10.2

$q = p_B - p_{K_1} = p_{\ell^+} + p_{\ell^-}$. The auxiliary functions $\mathcal{A}^{K_1}(\hat{s}), \dots, \mathcal{H}^{K_1}(\hat{s})$ are listed in the Appendix for convenience.

The dilepton invariant mass spectrum of the lepton pair for the $\bar{B} \rightarrow \bar{K}_1 \ell^+ \ell^-$ decay in the rest frame of the B meson is given by

$$\frac{d\Gamma(\bar{B} \rightarrow \bar{K}_1 \ell^+ \ell^-)}{d\hat{s}} = \frac{G_F^2 \alpha_{\text{em}}^2 m_B^5}{2^{12} \pi^5} |V_{tb} V_{ts}^*|^2 v \sqrt{\lambda} \Delta(\hat{s}), \quad (32)$$

where $v = \sqrt{1 - 4\hat{m}_\ell^2/\hat{s}}$, $\lambda = 1 + \hat{r}_{K_1}^2 + \hat{s}^2 - 2\hat{s} - 2\hat{r}_{K_1}(1 + \hat{s})$ and the definition of $\Delta(\hat{s})$ is presented in the Appendix.

The unpolarized and normalized differential forward-backward asymmetry of the $\bar{B} \rightarrow \bar{K}_1 \ell^+ \ell^-$ decay is defined by

$$\mathcal{A}_{\text{FB}} = \frac{\int_0^1 \frac{d^2\Gamma}{d\hat{s}dz} - \int_{-1}^0 \frac{d^2\Gamma}{d\hat{s}dz}}{\int_0^1 \frac{d^2\Gamma}{d\hat{s}dz} + \int_{-1}^0 \frac{d^2\Gamma}{d\hat{s}dz}}, \quad (33)$$

where $z = \cos \theta$ and θ is the angle between B meson and ℓ^- in the center of mass frame of leptons.

Using the definition mentioned above, the result can be written as follows:

$$\begin{aligned} \mathcal{A}_{\text{FB}}(\hat{s}) &= \frac{-2v\sqrt{\lambda}}{\hat{r}_{K_1}\Delta} \{2(\text{Re}[\mathcal{A}\mathcal{F}^*] + \text{Re}[\mathcal{B}\mathcal{E}^*])\hat{r}_{K_1}\hat{s} \\ &\quad + \hat{m}_\ell \text{Re}[\mathcal{B}(\mathcal{I}_1 + \mathcal{J}_1)^*](-1 + \hat{r}_{K_1} + \hat{s}) \\ &\quad + \hat{m}_\ell \text{Re}[\mathcal{C}(\mathcal{I}_1 + \mathcal{J}_1)^*]\lambda\}. \end{aligned} \quad (34)$$

At the end of this section, we place our attention on obtaining the normalized differential forward-backward asymmetries associated with the polarized leptons. For this purpose, we define the following orthogonal unit

$$\begin{aligned} \mathcal{A}_{\text{FB}}^{ij}(\hat{s}) &= \left(\frac{d\Gamma(\hat{s})}{d\hat{s}}\right)^{-1} \left\{ \int_0^1 dz - \int_{-1}^0 dz \right\} \left\{ \left[\frac{d^2\Gamma(\hat{s}, \vec{s}^- = \vec{i}, \vec{s}^+ = \vec{j})}{d\hat{s}dz} - \frac{d^2\Gamma(\hat{s}, \vec{s}^- = \vec{i}, \vec{s}^+ = -\vec{j})}{d\hat{s}dz} \right] \right. \\ &\quad \left. - \left[\frac{d^2\Gamma(\hat{s}, \vec{s}^- = -\vec{i}, \vec{s}^+ = \vec{j})}{d\hat{s}dz} - \frac{d^2\Gamma(\hat{s}, \vec{s}^- = -\vec{i}, \vec{s}^+ = -\vec{j})}{d\hat{s}dz} \right] \right\}, \\ &= \mathcal{A}_{\text{FB}}(\vec{s}^- = \vec{i}, \vec{s}^+ = \vec{j}) - \mathcal{A}_{\text{FB}}(\vec{s}^- = \vec{i}, \vec{s}^+ = -\vec{j}) - \mathcal{A}_{\text{FB}}(\vec{s}^- = -\vec{i}, \vec{s}^+ = \vec{j}) + \mathcal{A}_{\text{FB}}(\vec{s}^- = -\vec{i}, \vec{s}^+ = -\vec{j}), \end{aligned} \quad (37)$$

vectors $s_i^{\pm\mu}$ in the rest frame of ℓ^\pm , where $i = L, N$, and T are related to the longitudinal, normal, and transversal spin projections, respectively:

$$\begin{aligned} s_L^{-\mu} &= (0, \vec{e}_L^-) = \left(0, \frac{\vec{p}_{\ell^-}}{|\vec{p}_{\ell^-}|}\right), \\ s_N^{-\mu} &= (0, \vec{e}_N^-) = \left(0, \frac{\vec{p}_{K_1} \times \vec{p}_{\ell^-}}{|\vec{p}_{K_1} \times \vec{p}_{\ell^-}|}\right), \\ s_T^{-\mu} &= (0, \vec{e}_T^-) = (0, \vec{e}_N^- \times \vec{e}_L^-), \\ s_L^{+\mu} &= (0, \vec{e}_L^+) = \left(0, \frac{\vec{p}_{\ell^+}}{|\vec{p}_{\ell^+}|}\right), \\ s_N^{+\mu} &= (0, \vec{e}_N^+) = \left(0, \frac{\vec{p}_{K_1} \times \vec{p}_{\ell^+}}{|\vec{p}_{K_1} \times \vec{p}_{\ell^+}|}\right), \\ s_T^{+\mu} &= (0, \vec{e}_T^+) = (0, \vec{e}_N^+ \times \vec{e}_L^+), \end{aligned} \quad (35)$$

where \vec{p}_{ℓ^\mp} and \vec{p}_{K_1} are the three-momenta of the leptons ℓ^\mp and \bar{K}_1 meson in the center of mass frame (CM) of the $\ell^-\ell^+$ system, respectively. Using the Lorentz boost, the transformation of unit vectors from the rest frame of the leptons to the CM frame of leptons yields

$$\begin{aligned} (s_L^{\mp\mu})_{\text{CM}} &= \left(\frac{|\vec{p}_{\ell^\mp}|}{m_\ell}, \frac{E_\ell \vec{p}_{\ell^\mp}}{m_\ell |\vec{p}_{\ell^\mp}|}\right), \\ (s_N^{\mp\mu})_{\text{CM}} &= (s_N^{\mp\mu})_{\text{RF}}, \\ (s_T^{\mp\mu})_{\text{CM}} &= (s_T^{\mp\mu})_{\text{RF}}, \end{aligned} \quad (36)$$

where RF refers to the rest frame of the corresponding lepton as well as $\vec{p}_{\ell^+} = -\vec{p}_{\ell^-}$ and E_ℓ and m_ℓ are the energy and mass of leptons in the CM frame, respectively.

The definition of the polarized and normalized differential forward-backward asymmetry is

where $\frac{d\Gamma(\hat{s})}{d\hat{s}}$ is calculated in the CM frame. Using these definitions for the double polarized FB asymmetries, we get the following results:

$$\begin{aligned} \mathcal{A}_{\text{FB}}^{LL} &= \frac{-2v\sqrt{\lambda}}{\hat{r}_{K_1}\Delta} \{-2(\text{Re}[\mathcal{A}\mathcal{F}^*] + \text{Re}[\mathcal{B}\mathcal{E}^*])\hat{r}_{K_1}\hat{s} + \hat{m}_\ell \text{Re}[\mathcal{B}(\mathcal{I}_1 + \mathcal{J}_1)^*](-1 + \hat{r}_{K_1} + \hat{s}) \\ &\quad + \hat{m}_\ell \text{Re}[\mathcal{C}(\mathcal{I}_1 + \mathcal{J}_1)^*]\lambda\}, \end{aligned} \quad (38)$$

$$\begin{aligned} \mathcal{A}_{\text{FB}}^{LN} &= \frac{4v\lambda}{3\hat{r}_{K_1}\sqrt{\hat{s}}\Delta} \text{Im}[\hat{m}_\ell\lambda(\mathcal{C}\mathcal{G}^*) + \hat{m}_\ell(\mathcal{C}\mathcal{F}^*)(-1 + \hat{r}_{K_1} + \hat{s}) + \hat{m}_\ell(\mathcal{B}\mathcal{G}^*)(-1 + \hat{r}_{K_1} + \hat{s}) \\ &\quad + \hat{m}_\ell(\mathcal{B}\mathcal{F}^*) - \hat{m}_\ell\hat{s}\hat{r}_{K_1}(\mathcal{A}\mathcal{E}^*)], \end{aligned} \quad (39)$$

$$\mathcal{A}_{\text{FB}}^{NL} = \mathcal{A}_{\text{FB}}^{LN}, \quad (40)$$

$$\mathcal{A}_{\text{FB}}^{LT} = \frac{4\lambda}{3\hat{r}_{K_1}\sqrt{\hat{s}}\Delta} [\hat{m}_\ell\lambda|\mathcal{C}|^2 + 2\hat{m}_\ell \text{Re}[\mathcal{B}\mathcal{C}^*](-1 + \hat{r}_{K_1} + \hat{s}) + \hat{m}_\ell|\mathcal{B}|^2 - \hat{m}_\ell\hat{s}\hat{r}_{K_1}|A|^2], \quad (41)$$

$$\mathcal{A}_{\text{FB}}^{TL} = \mathcal{A}_{\text{FB}}^{LT}, \quad (42)$$

$$\begin{aligned} \mathcal{A}_{\text{FB}}^{NT} &= \frac{2\sqrt{\lambda}}{\hat{r}_{K_1}\hat{s}\Delta} \text{Im}[-2\hat{m}_\ell^2\lambda(\mathcal{C}\mathcal{G}^*)(1 - \hat{r}_{K_1}) + 2\hat{m}_\ell^2\lambda(\mathcal{C}\mathcal{F}^*) + 2\hat{m}_\ell^2(\mathcal{B}\mathcal{G}^*)(1 - \hat{r}_{K_1})(1 - \hat{r}_{K_1} - \hat{s}) \\ &\quad - 2\hat{m}_\ell^2(\mathcal{B}\mathcal{F}^*)(1 - \hat{r}_{K_1} - \hat{s}) - 2\hat{m}_\ell^2\hat{s}\lambda(\mathcal{C}\mathcal{H}^*) + 2\hat{m}_\ell^2\hat{s}(\mathcal{B}\mathcal{H}^*)(1 - \hat{r}_{K_1} - \hat{s}) \\ &\quad + \hat{m}_\ell\hat{s}(\mathcal{B}\mathcal{I}_2^*)(1 - 3\hat{r}_{K_1} - \hat{s}) + \hat{m}_\ell\hat{s}(\mathcal{B}\mathcal{J}_2^*)(1 - \hat{r}_{K_1} - \hat{s}) - \hat{m}_\ell\hat{s}\lambda(\mathcal{C}\mathcal{I}_2^*) - \hat{m}_\ell\hat{s}\lambda(\mathcal{C}\mathcal{J}_2^*)], \end{aligned} \quad (43)$$

$$\mathcal{A}_{\text{FB}}^{TN} = -\mathcal{A}_{\text{FB}}^{NT}, \quad (44)$$

$$\mathcal{A}_{\text{FB}}^{NN} = \frac{2v\sqrt{\lambda}}{\hat{r}_{K_1}\Delta} \text{Re}[\hat{m}_\ell\lambda\mathcal{C}(\mathcal{I}_1^* + \mathcal{J}_1^*) + \hat{m}_\ell\mathcal{B}(\mathcal{I}_1^* + \mathcal{J}_1^*)(-1 + \hat{r}_{K_1} + \hat{s})], \quad (45)$$

$$\mathcal{A}_{\text{FB}}^{TT} = \mathcal{A}_{\text{FB}}^{NN}. \quad (46)$$

E. Formulas of observables for $\bar{B} \rightarrow \bar{K}^* \ell^+ \ell^-$

Assuming $m_s = 0$ in the definitions of the form factors for $\bar{B} \rightarrow \bar{K}_1 \ell^+ \ell^-$ and $\bar{B} \rightarrow \bar{K}^* \ell^+ \ell^-$, we could derive the similar expressions for $\bar{B} \rightarrow \bar{K}^* \ell^+ \ell^-$ decay, such that all

the above equations remain unchanged except the definitions of the auxiliary functions [Eqs. (A1)–(A11)]. These definitions generally change by the following replacements:

$$\begin{aligned} -iA^{K_1} &\rightarrow V^{K^*}, & V_1^{K_1} &\rightarrow iA_1^{K^*}, & V_2^{K_1} &\rightarrow iA_2^{K^*}, & (V_3^{K_1} - V_0^{K_1}) &\rightarrow i(A_3^{K^*} - A_0^{K^*}), \\ V_0^{K_1} &\rightarrow iA_0^{K^*}, & T_1^{K_1} &\rightarrow iT_1^{K^*}, & -iT_2^{K_1} &\rightarrow T_2^{K^*}, & -iT_3^{K_1} &\rightarrow T_3^{K^*}. \end{aligned} \quad (47)$$

III. NUMERICAL RESULTS AND DISCUSSION

In this section we shall calculate the SM predictions and the sensitivities to the new physics due to model III of 2HDM for the polarized and unpolarized forward-backward asymmetries and their averages for $\bar{B} \rightarrow \bar{K}_1 \ell^+ \ell^-$ and $\bar{B} \rightarrow \bar{K}^* \ell^+ \ell^-$ decays. At the end, we compare the results of different decay modes to each other. The corresponding averages are defined by the following formula:

$$\langle A_{ij} \rangle = \frac{\int_{4\hat{m}_\ell^2}^{(1-\sqrt{\hat{r}_M})^2} A_{ij} \frac{d\mathcal{B}}{d\hat{s}} d\hat{s}}{\int_{4\hat{m}_\ell^2}^{(1-\sqrt{\hat{r}_M})^2} \frac{d\mathcal{B}}{d\hat{s}} d\hat{s}}, \quad (48)$$

where the subscript M stands for \bar{K}_1 and \bar{K}^* mesons. The full kinematical interval of the dilepton invariant mass q^2 is $4m_\ell^2 \leq q^2 \leq (m_B - m_M)^2$ for which the long distance effects (the charmonium resonances) can give significant

TABLE III. List of the values for the masses of the Higgs particles.

	m_{H^\pm} (GeV)	m_{A^0} (GeV)	m_{h^0} (GeV)	m_{H^0} (GeV)
Mass set-1	200	125	125	160
Mass set-2	160	125	125	160
Mass set-3	200	125	125	125
Mass set-4	160	125	125	125

contribution by including the first and the second resonances J/ψ and ψ' , in the interval of $8 \text{ GeV}^2 \leq q^2 \leq 14 \text{ GeV}^2$. In order to reduce the hadronic uncertainties we divide the kinematical region of q^2 for the muon as

- I $4m_\ell^2 \leq q^2 \leq (m_{J/\psi} - 0.02 \text{ GeV})^2$,
- II $(m_{J/\psi} + 0.02 \text{ GeV})^2 \leq q^2 \leq (m_{\psi'} - 0.02 \text{ GeV})^2$,
- III $(m_{\psi'} + 0.02 \text{ GeV})^2 \leq q^2 \leq (m_B - m_M)^2$,

and for tau as

- I $4m_\ell^2 \leq q^2 \leq (m_{\psi'} - 0.02 \text{ GeV})^2$,
- II $(m_{\psi'} + 0.02 \text{ GeV})^2 \leq q^2 \leq (m_B - m_M)^2$.

Since in model III of 2HDM, λ_{tt} and λ_{bb} can be complex parameters, we can rewrite the following product as

$$\lambda_{tt}\lambda_{bb} \equiv |\lambda_{tt}\lambda_{bb}|e^{i\theta}, \quad (49)$$

where $|\lambda_{tt}|$, $|\lambda_{bb}|$, and the phase angle θ are restricted by the experimental results of the electric dipole moments of the neutron (NEDM), $B^0 - \bar{B}^0$ mixing, ρ_0 , R_b , and $\text{Br}(b \rightarrow s\gamma)$ [10,12,19,20]. The experimental limits on NEDM and $\text{Br}(b \rightarrow s\gamma)$, plus M_{H^\pm} which is obtained at LEP II, put constraints on $\lambda_{tt}\lambda_{bb}$ to be nearly 1 and the phase angle θ to be in the interval $60^\circ - 90^\circ$. The experimental value of x_d

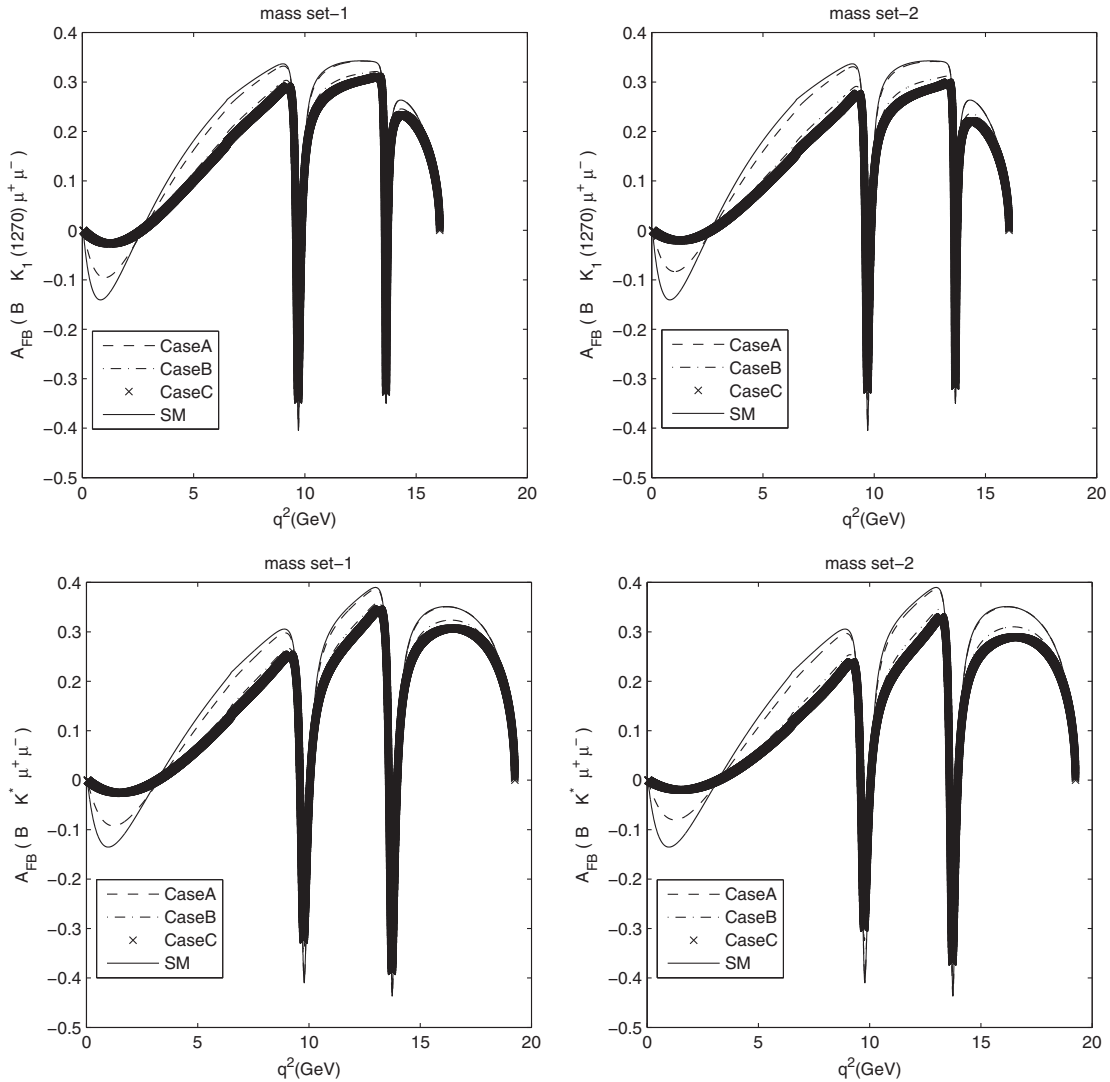


FIG. 1. The dependence of the A_{FB} polarization on q^2 and the three typical cases of 2HDM, i.e., cases A, B, and C, and SM for the μ channel of $\bar{B} \rightarrow \bar{K}_1$ and $\bar{B} \rightarrow \bar{K}^*$ transitions for the two typical mass sets 1 and 2.

parameter, relating to $B^0 - \bar{B}^0$ mixing, imposes the following restriction on $|\lambda_{tt}|$ which is $|\lambda_{tt}| \leq 0.3$. Also, the parameter R_b , which is defined as $R_b \equiv \frac{\Gamma(Z \rightarrow b\bar{b})}{\Gamma(Z \rightarrow \text{hadrons})}$, keeps $|\lambda_{bb}|$ approximately fixed, $|\lambda_{bb}| \approx 50$. Using these restrictions and taking $\theta = \pi/2$, we consider the following three typical parameter cases throughout the numerical analysis:

$$\begin{aligned} \text{A: } & |\lambda_{tt}| = 0.03; & |\lambda_{bb}| = 100, \\ \text{B: } & |\lambda_{tt}| = 0.15; & |\lambda_{bb}| = 50, \\ \text{C: } & |\lambda_{tt}| = 0.3; & |\lambda_{bb}| = 30. \end{aligned} \quad (50)$$

The other main input parameters are the form factors which are listed in Tables IV–XI. Also the magnitude of the mixing angle θ_{K_1} was estimated to be $|\theta_{K_1}| \approx 34^\circ \vee 57^\circ$ in

Ref. [21], $35^\circ \leq |\theta_{K_1}| \leq 55^\circ$ in Ref. [22], $|\theta_{K_1}| = 37^\circ \vee 58^\circ$ in Ref. [23], and $\theta_{K_1} = -(34 \pm 13)^\circ$ in [1,24]. In this study, we use the results of Refs. [1,24] for numerical calculations, where we take $\theta_{K_1} = -34^\circ$. In addition, in our numerical analysis we have used four sets of masses of Higgs bosons which are displayed in Table III.

We have presented our analysis for the dependency of A_{ij} 's and their averages on the parameters of model III of 2HDM in a series of Figures 1–11 and Tables IV–XI, respectively. In addition, in the aforementioned tables the theoretical and experimental uncertainties due to the SM averages of polarized and unpolarized forward-backward asymmetries in $\bar{B} \rightarrow \bar{K}_1 \ell^+ \ell^-$ and $\bar{B} \rightarrow \bar{K}^* \ell^+ \ell^-$ decays are considered. It should also be mentioned finally that the theoretical uncertainties come from the hadronic uncertainties related to the form factors and the experimental uncertainties originate from the mass of quarks and hadrons

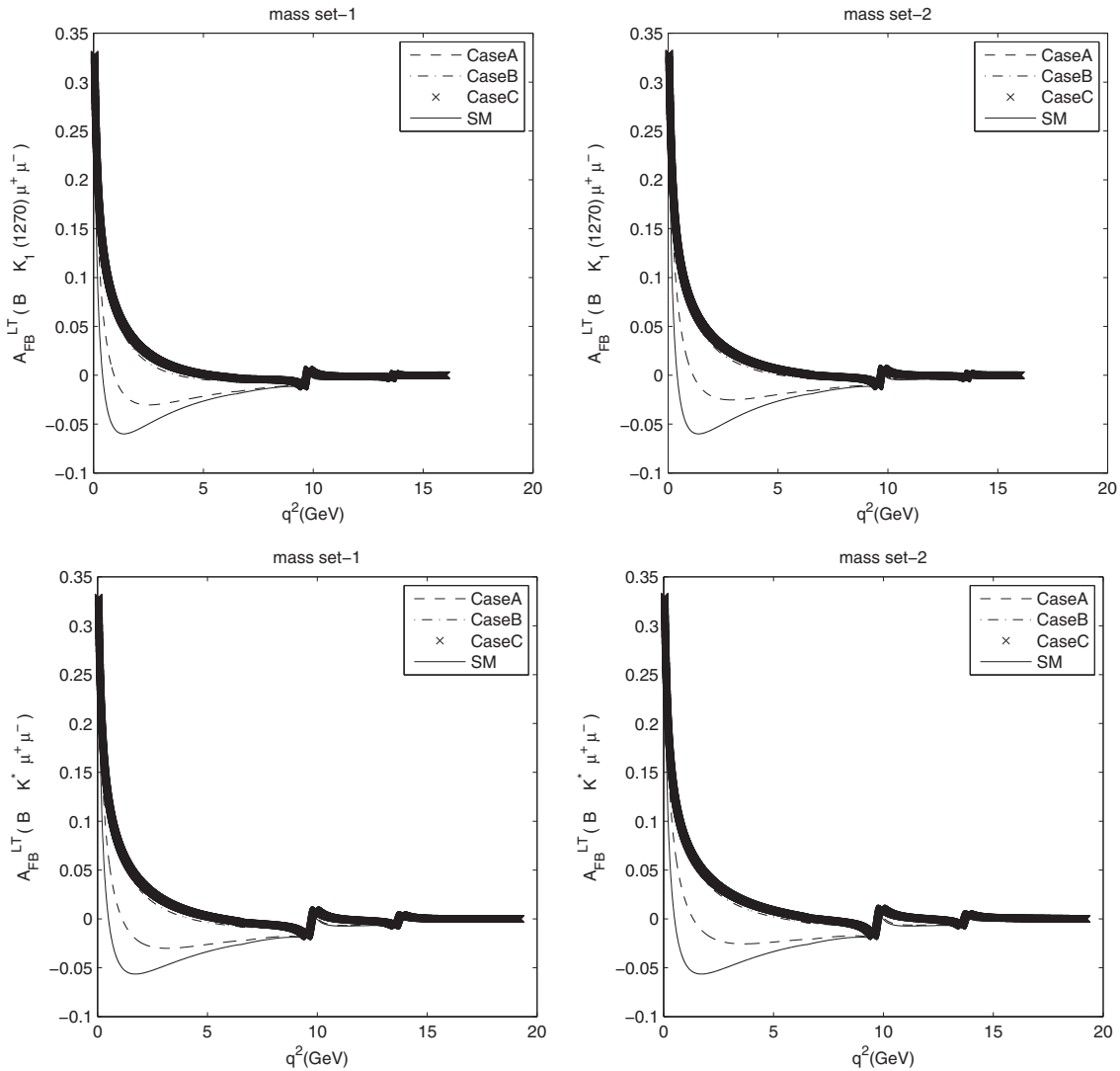


FIG. 2. The dependence of the A_{FB}^{LT} polarization on q^2 and the three typical cases of 2HDM, i.e., cases A, B, and C, and SM for the μ channel of $\bar{B} \rightarrow \bar{K}_1$ and $\bar{B} \rightarrow \bar{K}^*$ transitions for the two typical mass sets 1 and 2.

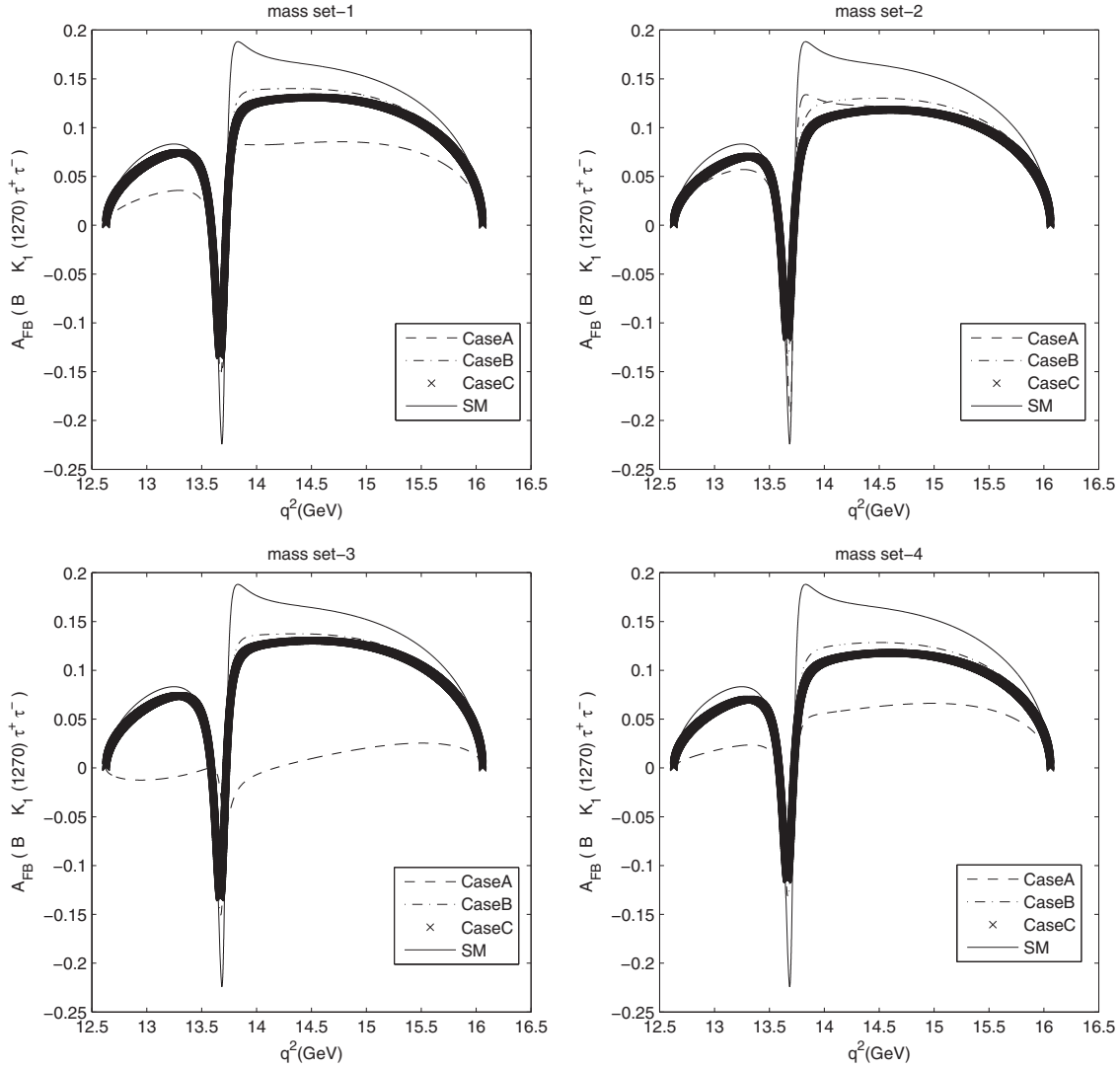


FIG. 3. The dependence of the A_{FB} polarization on q^2 and the three typical cases of 2HDM, i.e., cases A, B, and C, and SM for the τ channel of the $\bar{B} \rightarrow \bar{K}_1$ transition for the mass sets 1, 2, 3, and 4.

and Wolfenstein parameters. In the following analyses we have just talked about the asymmetries whose estimations are larger than 0.005 in 2HDM.

- (i) *Analysis of A_{FB} and A_{FB}^{LL} asymmetries for $\bar{B} \rightarrow \bar{K}_1 \mu^+ \mu^-$ and $\bar{B} \rightarrow \bar{K}^* \mu^+ \mu^-$ decays:* It is obvious from Tables IV and V that the predictions of both mass sets 1 and 3 and both mass sets 2 and 4 are separately the same for the unpolarized forward-backward asymmetry, A_{FB} , of $\bar{B} \rightarrow \bar{K}_1 \mu^+ \mu^-$ decay. Based on this, in Fig. 1 we have only presented the plots related to the mass sets 1 and 2. Also it is understood from the above discussion that the unpolarized A_{FB} for the mentioned decay shows an ignorable sensitivity to the change of mass of H^0 . In addition it is evident from these tables that the predictions of cases B and C have not lain on the SM interval such that the maximum deviation from the SM prediction is $-63\%SM$, which arises in case C.

Moreover, these tables show that the values of A^{LL} and the quality of their variations in SM and 2HDM are similar to those of A_{FB} . Considering this similarity, the plots related to A^{LL} have not been shown. Besides it is obvious from Fig. 1 and Tables VI and VII that the predictions of A_{FB} and A^{LL} for $\bar{B} \rightarrow \bar{K}^* \mu^+ \mu^-$ are to a large extent the same as those of $\bar{B} \rightarrow \bar{K}_1 \mu^+ \mu^-$ decay. Therefore, experimental study of this observable for the μ channel of $\bar{B} \rightarrow \bar{K}_1$ and $\bar{B} \rightarrow \bar{K}^*$ transitions can be useful in looking for new Higgs bosons.

- (ii) *Analysis of A_{FB}^{LT} asymmetries for $\bar{B} \rightarrow \bar{K}_1 \mu^+ \mu^-$ and $\bar{B} \rightarrow \bar{K}^* \mu^+ \mu^-$ decays:* Using Tables IV and V, it is apparent for the A^{LT} asymmetry of $\bar{B} \rightarrow \bar{K}_1 \mu^+ \mu^-$ decay that the expectation values of both mass sets 1 and 3 and both mass sets 2 and 4 are independently the same. Based on this, in Fig. 2 we have only presented the plots corresponding to mass sets 1 and

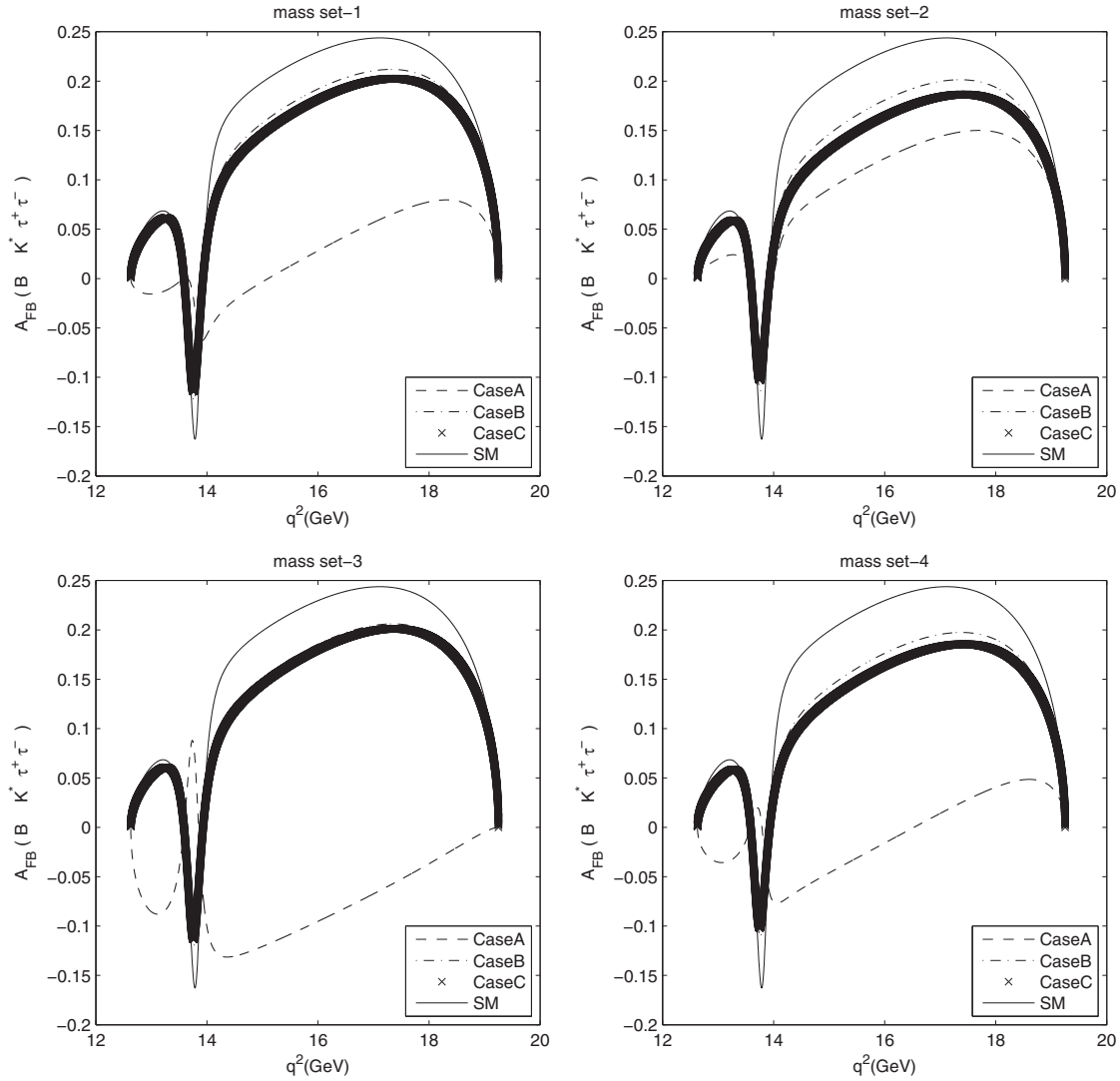


FIG. 4. The dependence of the A_{FB} polarization on q^2 and the three typical cases of 2HDM, i.e., cases A, B, and C, and SM for the τ channel of the $\bar{B} \rightarrow \bar{K}^*$ transition for mass sets 1, 2, 3, and 4.

2. Also it is understood from the above discussion that this asymmetry is insensitive to the variation of mass of H^0 for the mentioned decay. Furthermore, it is found out from the relevant tables that the anticipations of all mass sets and cases except for case A of mass sets 1 and 3 have extended in the range of the SM prediction. The maximum deviation relative to the SM prediction happens in case C which is closely -7 times of the SM prediction. In addition, the two Higgs doublet scenario may flip the sign of A^{LT} compared to the SM expectation. Moreover, it is clear from Fig. 2 and Tables VI and VII that the predictions of A^{LT} for $\bar{B} \rightarrow \bar{K}^* \mu^+ \mu^-$ look extremely similar to those of $\bar{B} \rightarrow \bar{K}_1 \mu^+ \mu^-$ decay, except that case A of mass sets 1 and 3 has not lain on the SM range. Therefore, it seems that the measurements of the sign and the magnitude of A^{LT}

for both mentioned decays could provide an appropriate way to discover new Higgs bosons.

- (iii) *Analysis of A_{FB} and A_{FB}^{LL} asymmetries for $\bar{B} \rightarrow \bar{K}_1 \tau^+ \tau^-$ and $\bar{B} \rightarrow \bar{K}^* \tau^+ \tau^-$ decays:* For the unpolarized forward-backward asymmetry, A_{FB} , the values of Tables VIII and IX indicate that only for cases B and C the predictions of mass set 1 resemble those of mass set 3 and likewise the predictions of mass set 2 resemble those of mass set 4. For case A, this claim is not valid anymore and the predictions of different mass sets are different from each other, such that a comparison between mass sets 1 and 3 and a comparison between mass sets 2 and 4 express that case A shows sensitivity to the change of mass of H^0 . For example, having decreased the mass of H^0 , the deviation from the SM has been increased. Based on this, in Fig. 3 we

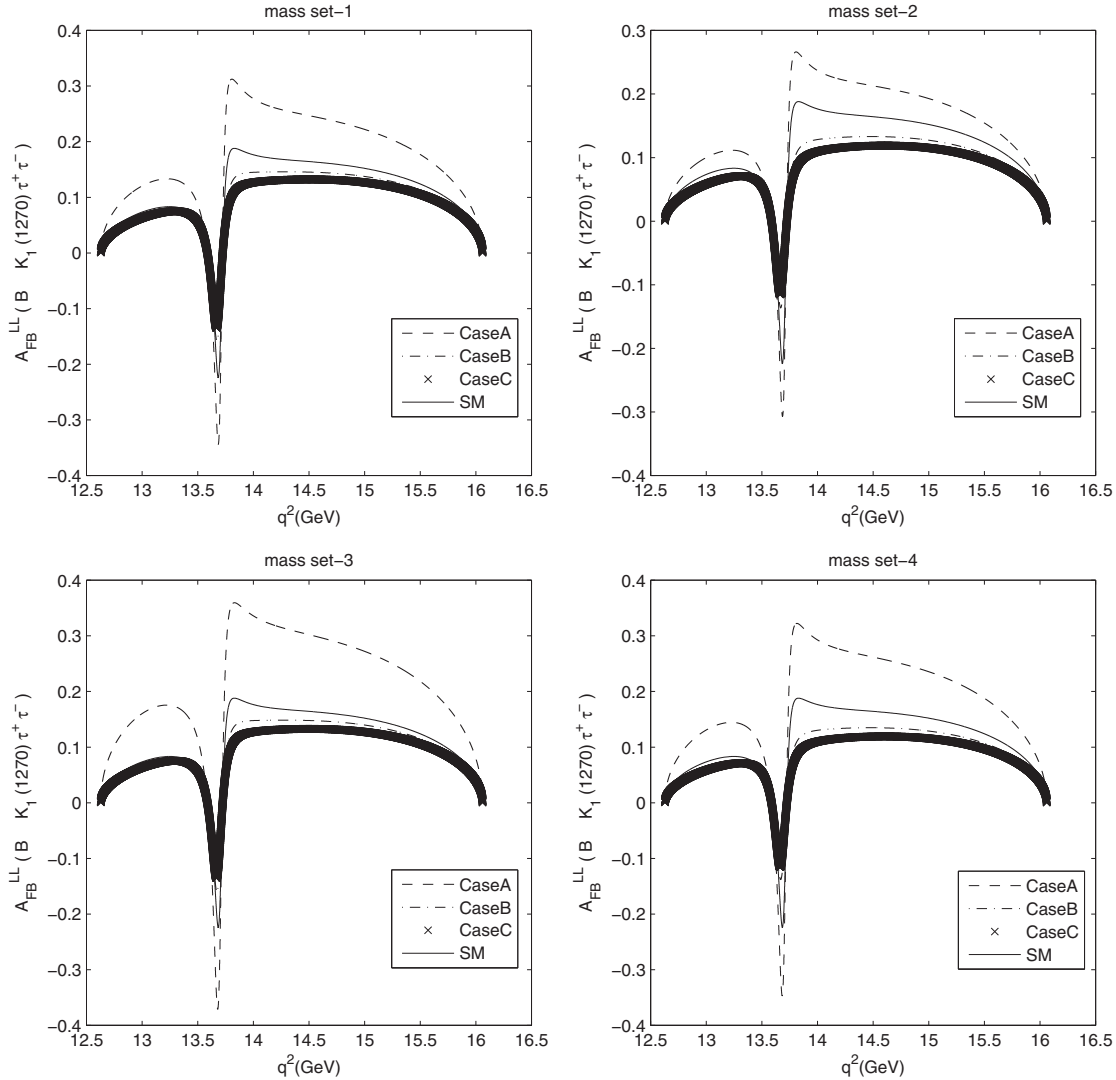


FIG. 5. The dependence of the A_{FB}^{LL} polarization on q^2 and the three typical cases of 2HDM, i.e., cases A, B and C, and SM for the τ channel of the $\bar{B} \rightarrow \bar{K}_1$ transition for the mass sets 1, 2, 3, and 4.

have presented the plots corresponding to whole mass sets. It is also found out through the above-mentioned tables that while there exist the expectations of cases B and C for all the mass sets in the SM interval, the predictions of case A for mass sets 1, 3, and 4 do not exist in the SM range. These predictions are smaller than the low limit of the SM anticipation; the maximum possible reduction is -100% of the SM value. Generally it is seen from Tables VIII and IX and Figs. 3 and 5 whereas both asymmetries A_{FB} and A^{LL} overlap each other to a large extent in the SM and in cases B and C, they differ from each other in case A. It is also found out from the mentioned tables that the predictions of A^{LL} in case A for mass sets 1, 3, and 4 are larger than the upper limit of the SM anticipation; the maximum possible enhancement is almost 2 times that of the SM amount. Also, it is evident from Tables X and XI

that there are similar explanations to the above expressions for the A_{FB} as well as A^{LL} asymmetries of the τ channel of the $\bar{B} \rightarrow \bar{K}^*$ transition. With regard to this point in Fig. 4 we have presented the plots corresponding to all mass sets. It is also understood from the corresponding tables that the same as before, the predictions of A_{FB} in case A for mass sets 1, 3, and 4 are smaller than the lower limit of the SM anticipation such that the maximum possible decrease is -140% of the SM value. In spite of this similarity, a comparison between the tabular data related to $\bar{B} \rightarrow \bar{K}^*$ and $\bar{B} \rightarrow \bar{K}_1$ transitions indicates that while a sign change could happen for the A_{FB} of $\bar{B} \rightarrow \bar{K}^* \tau^+ \tau^-$ decay, it does not occur for $\bar{B} \rightarrow \bar{K}_1 \tau^+ \tau^-$ decay. This asymmetry could only come down next to zero in the latter decay. Furthermore it is found out from the relevant tables that the same as before, the predictions of A^{LL}

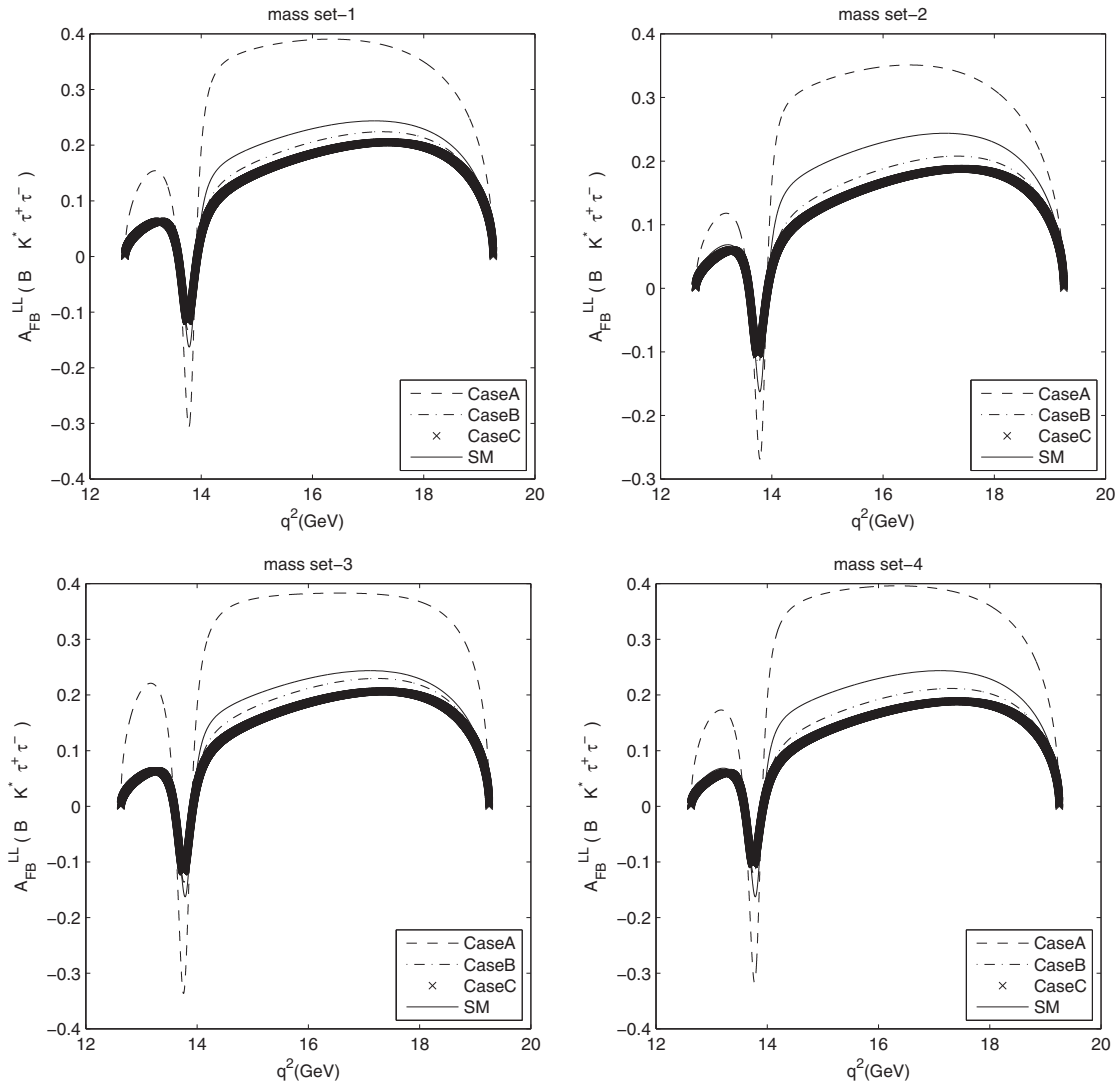


FIG. 6. The dependence of the A_{FB}^{LL} polarization on q^2 and the three typical cases of 2HDM, i.e., cases A, B, and C, and SM for the τ channel of the $\bar{B} \rightarrow \bar{K}^*$ transition for the mass sets 1, 2, 3, and 4.

in case A for mass sets 1, 3, and 4 are larger than the upper limit of the SM anticipation such that the maximum possible enhancement is nearly 2 times that of the SM amount. Also, any sign change is not observed for A^{LL} . Therefore, our results show that the sign and magnitude of A_{FB} and A^{LL} , for the τ channel of $\bar{B} \rightarrow \bar{K}_1$ and $\bar{B} \rightarrow \bar{K}^*$ transitions, could give testable evidence in establishing new Higgs bosons indirectly.

- (iv) *Analysis of A_{FB}^{NN} asymmetries for $\bar{B} \rightarrow \bar{K}_1 \tau^+ \tau^-$ and $\bar{B} \rightarrow \bar{K}^* \tau^+ \tau^-$ decays:* It is revealed from formula (45) and Tables VIII and IX for $\bar{B} \rightarrow \bar{K}_1 \tau^+ \tau^-$ decay that whereas the SM anticipation for A^{NN} is exactly zero, the order of data in cases B and C for all mass sets is of the order of 10^{-3} and in case A varies from the order of 10^{-2} to 10^{-1} for various mass sets. The largest deviation from the SM value is seen in case A of mass set 3, in which the smallest mass of H^0 and

the biggest mass of H^\pm are considered. It is also obvious from the corresponding tables that the predictions of case A do not lie on the SM expectation. Since there exist some large discrepancies between the predictions of different mass sets in case A, we have presented the related entire plots in Fig. 7. Moreover it is found out from Tables X and XI that there are similar findings regarding the latter decay and the former decay. In this regard the relevant plots are given in Fig. 8. The mere exception is that while the orders of cases A and C remain unchanged compared to those of the former decay, the order of case B changes such that this order becomes between 10^{-3} and 10^{-2} . Therefore, study of this observable in the experiments, for the τ channel of $\bar{B} \rightarrow \bar{K}_1$ and $\bar{B} \rightarrow \bar{K}^*$ transitions, can give promising information about the existence of new Higgs bosons.

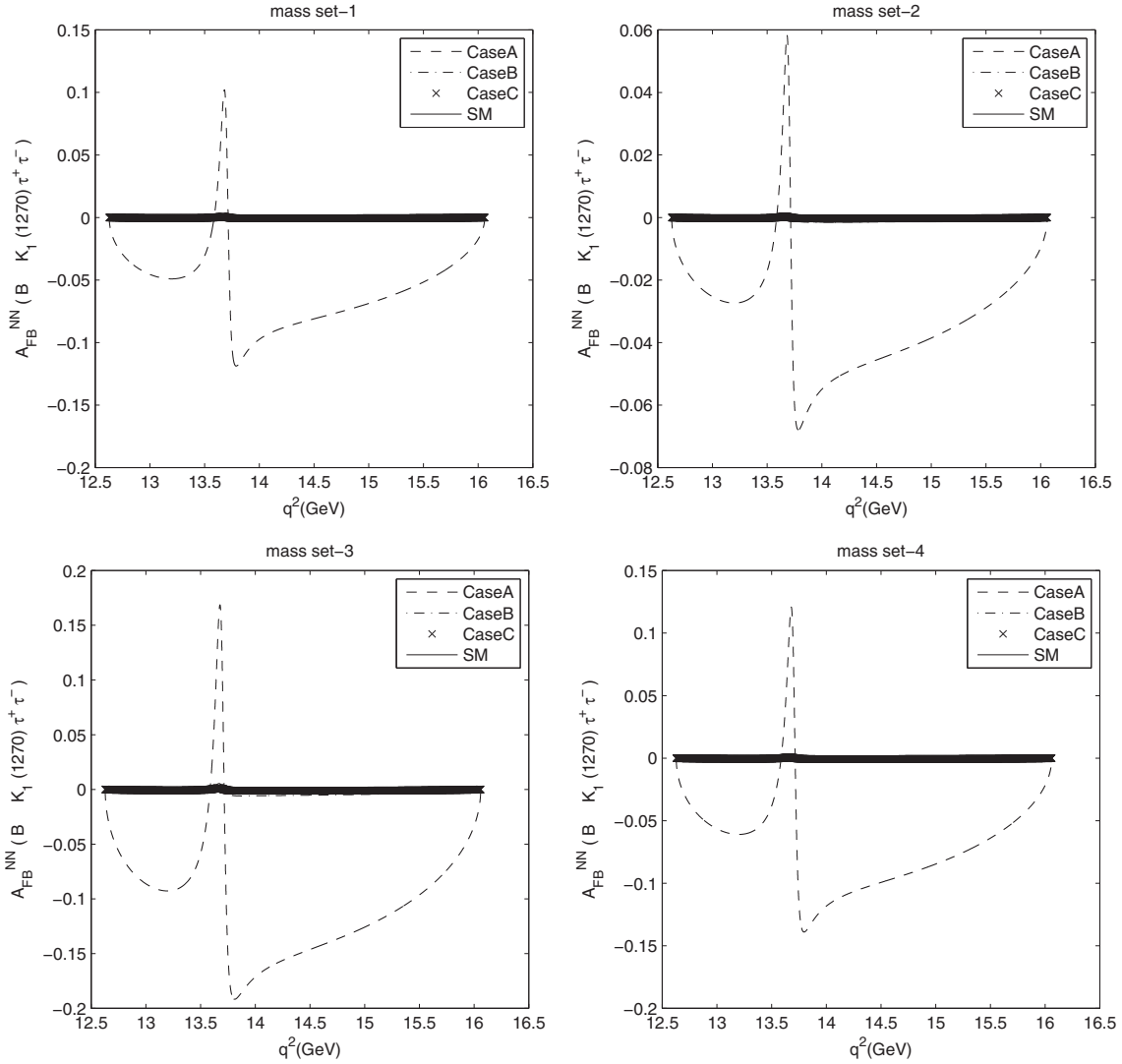


FIG. 7. The dependence of the A_{FB}^{NN} polarization on q^2 and the three typical cases of 2HDM, i.e., cases A, B and C, and SM for the τ channel of the $\bar{B} \rightarrow \bar{K}_1$ transition for the mass sets 1, 2, 3, and 4.

(v) *Analysis of A_{FB}^{LN} asymmetries for $\bar{B} \rightarrow \bar{K}_1\tau^+\tau^-$ and $\bar{B} \rightarrow \bar{K}^*\tau^+\tau^-$ decays:* From Tables VIII and IX, it becomes apparent that the predictions of A^{LN} in the SM and 2HDM for the τ channel of $\bar{B} \rightarrow \bar{K}_1$ transition are insignificant. So, they have been canceled from our discussion. In contrast, it is seen from Tables X and XI that except for the prediction of case A for mass sets 1 and 3, all the other predictions have not been placed in the SM range. Also, it is understood from the corresponding tables that while the predictions of cases B and C for all mass sets are identical and of the order of 10^{-3} , those of case A are different in various mass sets and their order varies from 10^{-3} to 10^{-2} . Therefore, investigation of this asymmetry in the experiments, for the latter decay, can provide a useful tool in establishing the presence of new Higgs bosons. The related diagrams are shown in Fig. 9.

(vi) *Analysis of A_{FB}^{LT} asymmetries for $\bar{B} \rightarrow \bar{K}_1\tau^+\tau^-$ and $\bar{B} \rightarrow \bar{K}^*\tau^+\tau^-$ decays:* Using Tables VIII and IX as well as X and XI, it is apparent for the A^{LT} asymmetry of each decay that the expectation values of mass set 1 look like those of mass set 3 and the expectation amounts of mass set 2 look like those of mass set 4. Moreover, these tabular data show that the anticipations of 2HDM for each of mass sets and cases are situated in the SM interval. The relevant diagrams are also drawn in Fig. 10. Based on the above discussion, the measurement of this asymmetry could not have any signs for finding new Higgs bosons.

(vii) *Analysis of A_{FB}^{NT} asymmetries for $\bar{B} \rightarrow \bar{K}_1\tau^+\tau^-$ and $\bar{B} \rightarrow \bar{K}^*\tau^+\tau^-$ decays:* It is evident through Tables VIII and IX that for the former decay the predictions of mass set 1 resemble those of mass set 3 and likewise the predictions of mass set 2 resemble

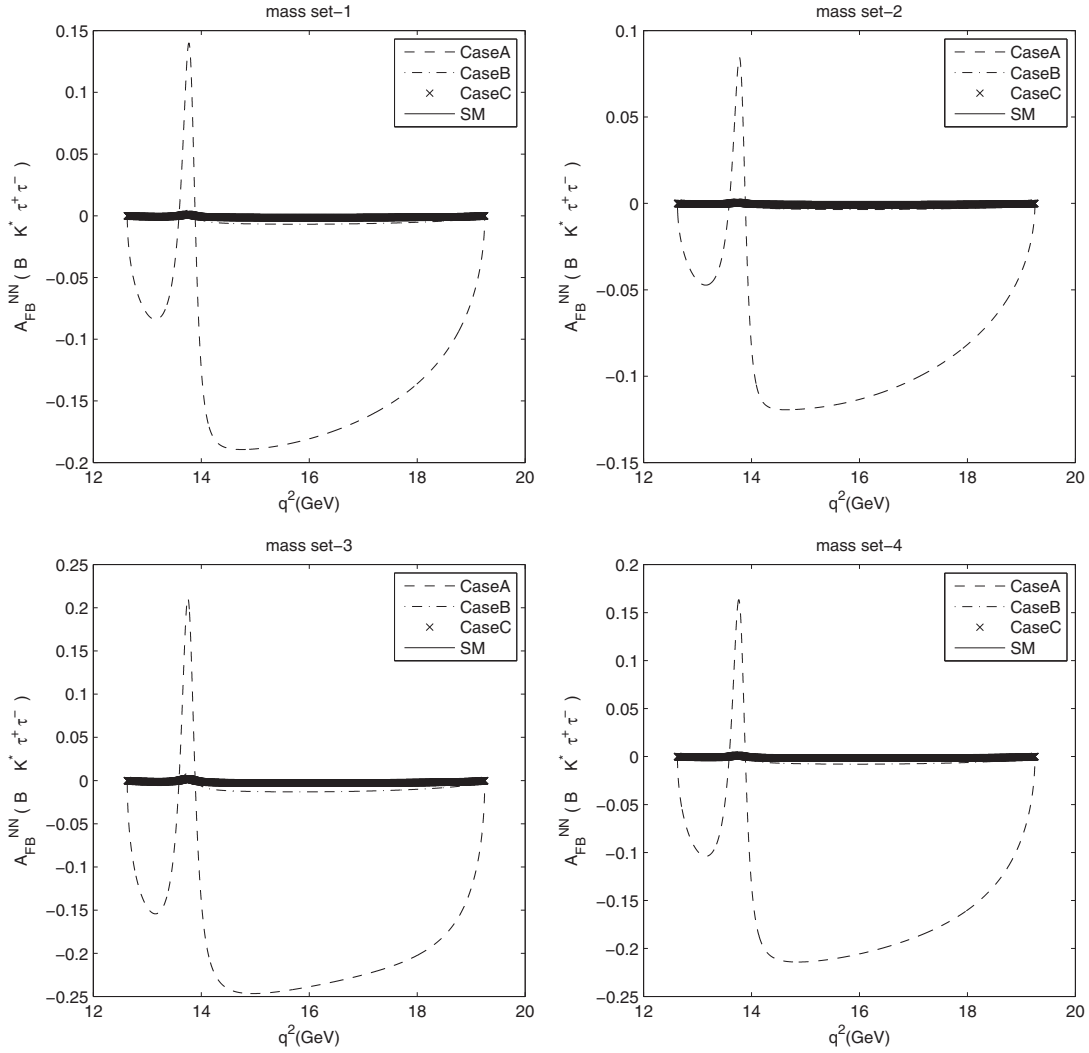


FIG. 8. The dependence of the A_{FB}^{NN} polarization on q^2 and the three typical cases of 2HDM, i.e., cases A, B, and C, and SM for the τ channel of the $\bar{B} \rightarrow \bar{K}^*$ transition for the mass sets 1, 2, 3, and 4.

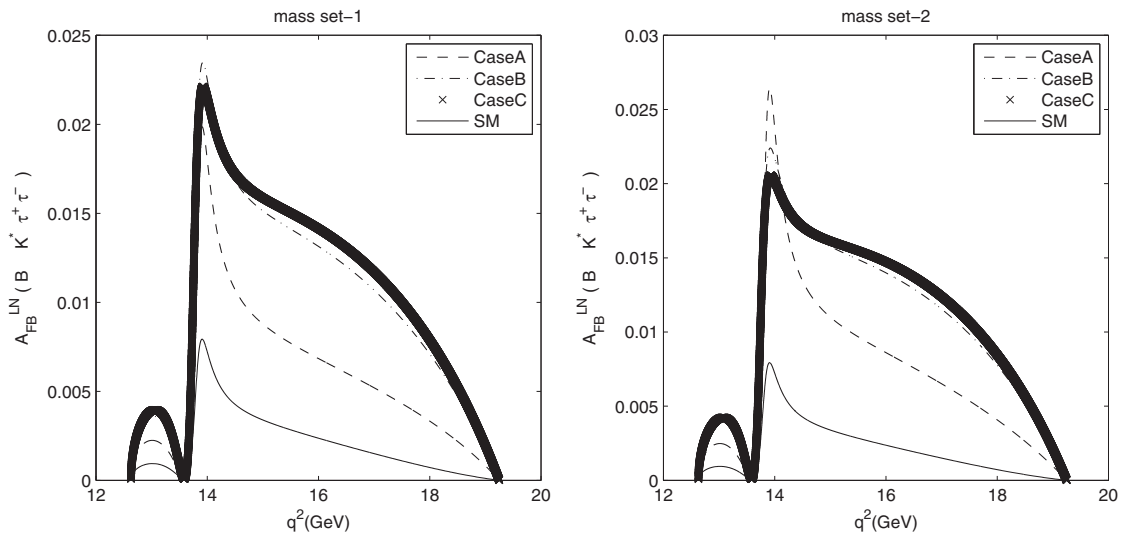


FIG. 9. The dependence of the A_{FB}^{LN} polarization on q^2 and the three typical cases of 2HDM, i.e., cases A, B, and C, and SM for the τ channel of the $\bar{B} \rightarrow \bar{K}^*$ transition for the two typical mass sets 1 and 2.

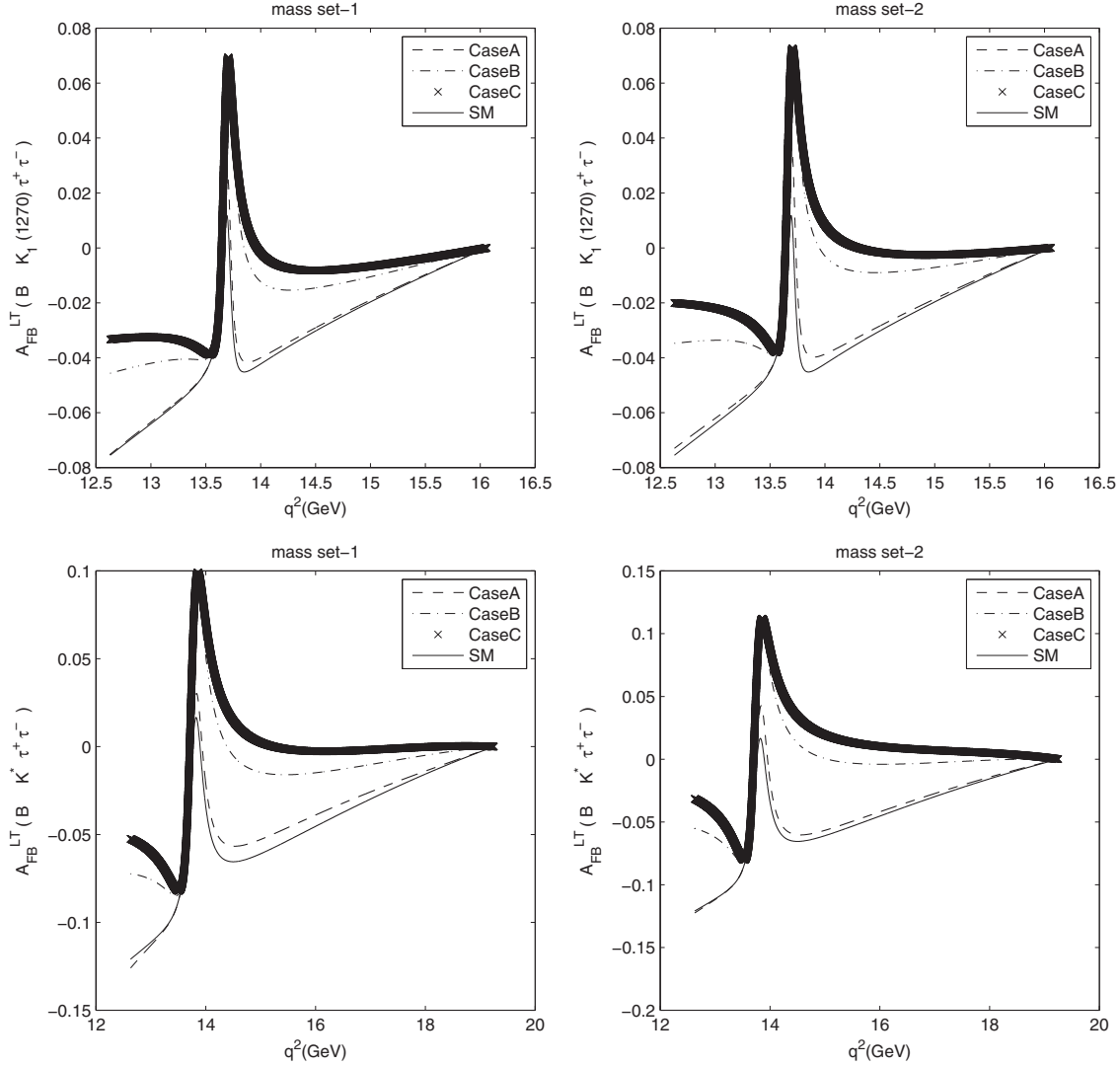


FIG. 10. The dependence of the A_{FB}^{LT} polarization on q^2 and the three typical cases of 2HDM, i.e., cases A, B, and C, and SM for the τ channel of $\bar{B} \rightarrow \bar{K}_1$ and $\bar{B} \rightarrow \bar{K}^*$ transitions for the two typical mass sets 1 and 2.

those of mass set 4. It is also revealed from the tables that the predictions of each of mass sets have not lain on the SM range. The maximum deviation from the SM prediction takes place in case C of mass sets 2 and 4 which is -3 times the SM prediction. In addition, while the anticipation of SM is entirely negative in its allowed region, those of 2HDM are completely positive in whole mass sets. It is also obvious from Tables X and XI that there are the same conditions regarding the latter decay. So, the measurements of the sign and magnitude of A^{NT} for the latter and the former decays can serve as good tests for discovering new Higgs bosons. The corresponding diagrams are depicted in Fig. 11.

Finally, let us discuss briefly whether the lepton polarization asymmetries are measurable in experiments or not. Experimentally, for measuring an asymmetry $\langle A_{ij} \rangle$ of the decay with branching ratio \mathcal{B} at $n\sigma$ level, the required

number of events (i.e., the number of $B\bar{B}$) is given by the formula

$$N = \frac{n^2}{\mathcal{B}s_1s_2\langle A_{ij} \rangle^2},$$

where s_1 and s_2 are the efficiencies of the leptons. The values of the efficiencies of the τ leptons differ from 50% to 90% for their various decay modes [25] and the error in τ -lepton polarization is approximately 10%–15% [26]. So, the error in measurements of the τ -lepton asymmetries is estimated to be about 20%–30%, and the error in obtaining the number of events is about 50%.

Based on the above expression for N , in order to detect the polarized and unpolarized forward-backward asymmetries in the μ and τ channels at 3σ level, the minimum number of required events are given by (the efficiency of the τ lepton is considered to be 0.5)

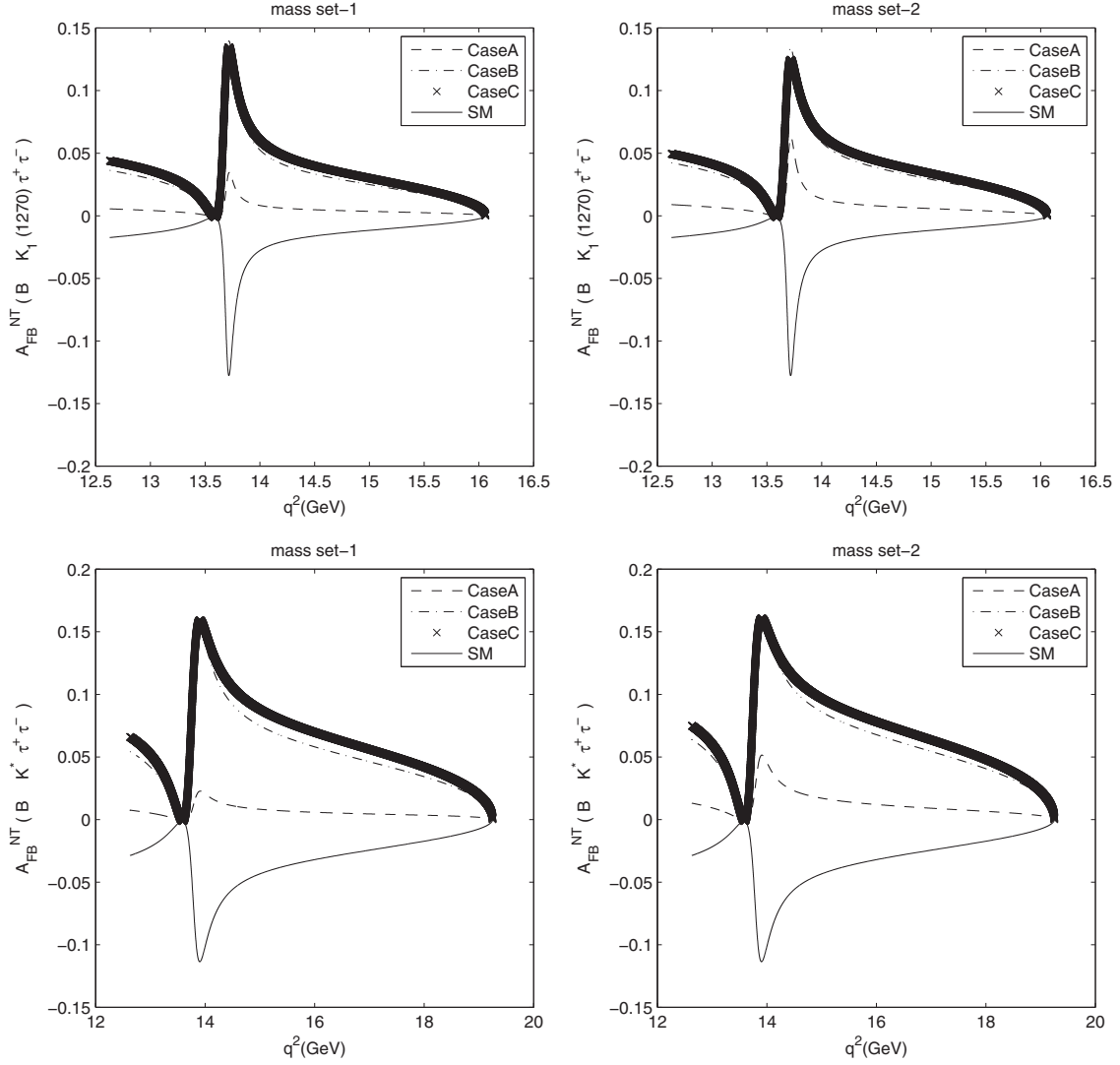


FIG. 11. The dependence of the A_{FB}^{NT} polarization on q^2 and the three typical cases of 2HDM, i.e., cases A, B, and C, and SM for the τ channel of $\bar{B} \rightarrow \bar{K}_1$ and $\bar{B} \rightarrow \bar{K}^*$ transitions for the two typical mass sets 1 and 2.

(i) for $\bar{B} \rightarrow \bar{K}_1 \mu^+ \mu^-$ decay

(ii) for $\bar{B} \rightarrow \bar{K}^* \mu^+ \mu^-$ decay

$$N \sim \begin{cases} 10^8 & \text{for } \langle A_{\text{FB}} \rangle, \\ 10^8 & \text{for } \langle A_{\text{FB}}^{LL} \rangle, \\ 10^{11} & \text{(for } \langle A_{\text{FB}}^{NN} \rangle, \langle A_{\text{FB}}^{TT} \rangle), \\ 10^{11} & \text{(for } \langle A_{\text{FB}}^{LN} \rangle, \langle A_{\text{FB}}^{NL} \rangle), \\ 10^8 & \text{(for } \langle A_{\text{FB}}^{LT} \rangle, \langle A_{\text{FB}}^{TL} \rangle), \\ 10^{12} & \text{(for } \langle A_{\text{FB}}^{NT} \rangle, \langle A_{\text{FB}}^{TN} \rangle), \end{cases}$$

$$N \sim \begin{cases} 10^8 & \text{for } \langle A_{\text{FB}} \rangle, \\ 10^8 & \text{for } \langle A_{\text{FB}}^{LL} \rangle, \\ 10^{12} & \text{(for } \langle A_{\text{FB}}^{NN} \rangle, \langle A_{\text{FB}}^{TT} \rangle), \\ 10^{12} & \text{(for } \langle A_{\text{FB}}^{LN} \rangle, \langle A_{\text{FB}}^{NL} \rangle), \\ 10^9 & \text{(for } \langle A_{\text{FB}}^{LT} \rangle, \langle A_{\text{FB}}^{TL} \rangle), \\ 10^{12} & \text{(for } \langle A_{\text{FB}}^{NT} \rangle, \langle A_{\text{FB}}^{TN} \rangle), \end{cases}$$

TABLE IV. The averaged unpolarized and polarized forward-backward asymmetries for $\bar{B} \rightarrow \bar{K}_1(1270)\mu^+\mu^-$ in SM and 2HDM for the mass sets 1 and 2 of Higgs bosons and the three cases A ($\theta = \pi/2$, $|\lambda_{tt}| = 0.03$, and $|\lambda_{bb}| = 100$), B ($\theta = \pi/2$, $|\lambda_{tt}| = 0.15$, and $|\lambda_{bb}| = 50$), and C ($\theta = \pi/2$, $|\lambda_{tt}| = 0.3$, and $|\lambda_{bb}| = 30$). The errors shown for each asymmetry are due to the theoretical and experimental uncertainties. The first ones are related to the theoretical uncertainties and the second ones are due to experimental uncertainties. The theoretical uncertainties come from the hadronic uncertainties related to the form factors and the experimental uncertainties originate from the mass of quarks and hadrons and Wolfenstein parameters.

	SM	Case A (Set 1)	Case B (Set 1)	Case C (Set 1)	Case A (Set 2)	Case B (Set 2)	Case C (Set 2)
$\langle A_{FB} \rangle$	$+0.196_{-0.051-0.003}^{+0.071+0.002}$	+0.170	+0.104	+0.087	+0.164	+0.088	+0.071
$\langle A_{FB}^{LL} \rangle$	$+0.196_{-0.051-0.003}^{+0.071+0.002}$	+0.173	+0.104	+0.087	+0.165	+0.088	+0.071
$\langle A_{FB}^{NN} \rangle$	$\pm 0.000_{-0.000-0.000}^{+0.000+0.000}$	-0.002	-0.000	-0.000	-0.001	-0.000	-0.000
$\langle A_{FB}^{LN} \rangle$	$+0.000_{-0.000-0.000}^{+0.000+0.000}$	+0.002	+0.002	+0.002	+0.002	+0.002	+0.002
$\langle A_{FB}^{LT} \rangle$	$-0.011_{-0.012-0.002}^{+0.017+0.002}$	+0.007	+0.056	+0.069	+0.013	+0.068	+0.080
$\langle A_{FB}^{NT} \rangle$	$-0.000_{-0.000-0.000}^{+0.000+0.000}$	+0.001	+0.001	+0.001	+0.001	+0.001	+0.001

TABLE V. The same as Table IV but for the mass sets 3 and 4 of Higgs bosons.

	SM	Case A (Set 3)	Case B (Set 3)	Case C (Set 3)	Case A (Set 4)	Case B (Set 4)	Case C (Set 4)
$\langle A_{FB} \rangle$	$+0.196_{-0.051-0.003}^{+0.071+0.002}$	+0.166	+0.104	+0.087	+0.161	+0.088	+0.071
$\langle A_{FB}^{LL} \rangle$	$+0.196_{-0.051-0.003}^{+0.071+0.002}$	+0.172	+0.104	+0.087	+0.165	+0.088	+0.071
$\langle A_{FB}^{NN} \rangle$	$\pm 0.000_{-0.000-0.000}^{+0.000+0.000}$	-0.003	-0.000	-0.000	-0.002	-0.000	-0.000
$\langle A_{FB}^{LN} \rangle$	$+0.000_{-0.000-0.000}^{+0.000+0.000}$	+0.002	+0.002	+0.002	+0.002	+0.002	+0.002
$\langle A_{FB}^{LT} \rangle$	$-0.011_{-0.012-0.002}^{+0.017+0.002}$	+0.007	+0.056	+0.069	+0.013	+0.068	+0.080
$\langle A_{FB}^{NT} \rangle$	$-0.000_{-0.000-0.000}^{+0.000+0.000}$	+0.001	+0.001	+0.001	+0.001	+0.001	+0.001

TABLE VI. The same as Table IV but for the $\bar{B} \rightarrow \bar{K}^*\mu^+\mu^-$.

	SM	Case A (Set 1)	Case B (Set 1)	Case C (Set 1)	Case A (Set 2)	Case B (Set 2)	Case C (Set 2)
$\langle A_{FB} \rangle$	$+0.192_{-0.061-0.003}^{+0.055+0.012}$	+0.165	+0.102	+0.084	+0.160	+0.086	+0.069
$\langle A_{FB}^{LL} \rangle$	$+0.192_{-0.061-0.003}^{+0.055+0.012}$	+0.169	+0.102	+0.084	+0.162	+0.086	+0.069
$\langle A_{FB}^{NN} \rangle$	$\pm 0.000_{-0.000-0.000}^{+0.000+0.000}$	-0.002	-0.000	-0.000	-0.001	-0.000	-0.000
$\langle A_{FB}^{LN} \rangle$	$+0.001_{-0.000-0.000}^{+0.000+0.000}$	+0.002	+0.002	+0.002	+0.002	+0.002	+0.002
$\langle A_{FB}^{LT} \rangle$	$-0.011_{-0.017-0.004}^{+0.013+0.003}$	+0.007	+0.055	+0.067	+0.013	+0.066	+0.078
$\langle A_{FB}^{NT} \rangle$	$-0.000_{-0.000-0.000}^{+0.000+0.000}$	+0.001	+0.001	+0.001	+0.001	+0.001	+0.001

TABLE VII. The same as Table VI except for the mass sets 3 and 4 of Higgs bosons.

	SM	Case A (Set 3)	Case B (Set 3)	Case C (Set 3)	Case A (Set 4)	Case B (Set 4)	Case C (Set 4)
$\langle A_{FB} \rangle$	$+0.192_{-0.061-0.003}^{+0.055+0.012}$	+0.161	+0.101	+0.084	+0.157	+0.086	+0.069
$\langle A_{FB}^{LL} \rangle$	$+0.192_{-0.061-0.003}^{+0.055+0.012}$	+0.168	+0.102	+0.084	+0.161	+0.086	+0.069
$\langle A_{FB}^{NN} \rangle$	$\pm 0.000_{-0.000-0.000}^{+0.000+0.000}$	-0.004	-0.000	-0.000	-0.002	-0.000	-0.000
$\langle A_{FB}^{LN} \rangle$	$+0.001_{-0.000-0.000}^{+0.000+0.000}$	+0.002	+0.002	+0.002	+0.002	+0.002	+0.002
$\langle A_{FB}^{LT} \rangle$	$-0.011_{-0.017-0.004}^{+0.013+0.003}$	+0.008	+0.055	+0.067	+0.013	+0.066	+0.078
$\langle A_{FB}^{NT} \rangle$	$-0.000_{-0.000-0.000}^{+0.000+0.000}$	+0.001	+0.001	+0.001	+0.001	+0.001	+0.001

TABLE VIII. The same as Table IV except for $\bar{B} \rightarrow \bar{K}_1 \tau^+ \tau^-$.

	SM	Case A (Set 1)	Case B (Set 1)	Case C (Set 1)	Case A (Set 2)	Case B (Set 2)	Case C (Set 2)
$\langle A_{FB} \rangle$	$+0.120^{+0.039+0.017}_{-0.025-0.014}$	+0.061	+0.104	+0.099	+0.088	+0.098	+0.091
$\langle A_{FB}^{LL} \rangle$	$+0.120^{+0.039+0.017}_{-0.025-0.014}$	+0.182	+0.109	+0.100	+0.156	+0.101	+0.091
$\langle A_{FB}^{NN} \rangle$	$\pm 0.000^{+0.000+0.000}_{-0.000-0.000}$	-0.061	-0.002	-0.000	-0.034	-0.001	-0.000
$\langle A_{FB}^{LN} \rangle$	$+0.001^{+0.001+0.000}_{-0.000-0.000}$	+0.002	+0.003	+0.003	+0.002	+0.003	+0.003
$\langle A_{FB}^{LT} \rangle$	$-0.036^{+0.023+0.006}_{-0.015-0.007}$	-0.035	-0.021	-0.014	-0.034	-0.015	-0.008
$\langle A_{FB}^{NT} \rangle$	$-0.013^{+0.005+0.001}_{-0.003-0.001}$	+0.004	+0.028	+0.034	+0.007	+0.033	+0.038

TABLE IX. The same as Table VIII but for the mass sets 3 and 4 of Higgs bosons.

	SM	Case A (Set 3)	Case B (Set 3)	Case C (Set 3)	Case A (Set 4)	Case B (Set 4)	Case C (Set 4)
$\langle A_{FB} \rangle$	$+0.120^{+0.039+0.017}_{-0.025-0.014}$	+0.005	+0.103	+0.100	+0.045	+0.097	+0.090
$\langle A_{FB}^{LL} \rangle$	$+0.120^{+0.039+0.017}_{-0.025-0.014}$	+0.229	+0.111	+0.101	+0.195	+0.102	+0.091
$\langle A_{FB}^{NN} \rangle$	$\pm 0.000^{+0.000+0.000}_{-0.000-0.000}$	-0.112	-0.004	-0.001	-0.075	-0.003	-0.001
$\langle A_{FB}^{LN} \rangle$	$+0.001^{+0.001+0.000}_{-0.000-0.000}$	+0.002	+0.003	+0.003	+0.002	+0.003	+0.003
$\langle A_{FB}^{LT} \rangle$	$-0.036^{+0.023+0.006}_{-0.015-0.007}$	-0.034	-0.021	-0.014	-0.034	-0.015	-0.008
$\langle A_{FB}^{NT} \rangle$	$-0.013^{+0.005+0.001}_{-0.003-0.001}$	+0.004	+0.028	+0.034	+0.007	+0.033	+0.038

TABLE X. The same as Table VI except for $\bar{B} \rightarrow \bar{K}^* \tau^+ \tau^-$.

	SM	Case A (Set 1)	Case B (Set 1)	Case C (Set 1)	Case A (Set 2)	Case B (Set 2)	Case C (Set 2)
$\langle A_{FB} \rangle$	$+0.177^{+0.031+0.058}_{-0.034-0.035}$	+0.027	+0.150	+0.142	+0.100	+0.142	+0.130
$\langle A_{FB}^{LL} \rangle$	$+0.177^{+0.031+0.058}_{-0.034-0.035}$	+0.308	+0.160	+0.145	+0.267	+0.147	+0.131
$\langle A_{FB}^{NN} \rangle$	$\pm 0.000^{+0.000+0.000}_{-0.000-0.000}$	-0.141	-0.005	-0.001	-0.085	-0.003	-0.001
$\langle A_{FB}^{LN} \rangle$	$+0.002^{+0.002+0.001}_{-0.002-0.003}$	+0.005	+0.010	+0.011	+0.010	+0.011	+0.011
$\langle A_{FB}^{LT} \rangle$	$-0.050^{+0.032+0.014}_{-0.037-0.029}$	-0.050	-0.021	-0.010	-0.047	-0.011	+0.003
$\langle A_{FB}^{NT} \rangle$	$-0.028^{+0.004+0.002}_{-0.004-0.000}$	+0.005	+0.052	+0.062	+0.011	+0.061	+0.070

TABLE XI. The same as Table X but for the mass sets 3 and 4 of Higgs bosons.

	SM	Case A (Set 3)	Case B (Set 3)	Case C (Set 3)	Case A (Set 4)	Case B (Set 4)	Case C (Set 4)
$\langle A_{FB} \rangle$	$+0.177^{+0.031+0.058}_{-0.034-0.035}$	-0.077	+0.145	+0.141	-0.008	+0.138	+0.129
$\langle A_{FB}^{LL} \rangle$	$+0.177^{+0.031+0.058}_{-0.034-0.035}$	+0.330	+0.165	+0.146	+0.320	+0.150	+0.132
$\langle A_{FB}^{NN} \rangle$	$\pm 0.000^{+0.000+0.000}_{-0.000-0.000}$	-0.204	-0.010	-0.002	-0.164	-0.006	-0.001
$\langle A_{FB}^{LN} \rangle$	$+0.002^{+0.002+0.001}_{-0.002-0.003}$	+0.004	+0.010	+0.011	+0.006	+0.011	+0.011
$\langle A_{FB}^{LT} \rangle$	$-0.050^{+0.032+0.014}_{-0.037-0.029}$	-0.034	-0.021	-0.010	-0.041	-0.011	+0.003
$\langle A_{FB}^{NT} \rangle$	$-0.028^{+0.004+0.002}_{-0.004-0.000}$	+0.004	+0.052	+0.062	+0.010	+0.061	+0.070

(iii) for $\bar{B} \rightarrow \bar{K}_1 \tau^+ \tau^-$ decay

$$N \sim \begin{cases} 10^{10} & \text{for } \langle A_{\text{FB}} \rangle, \\ 10^{10} & \text{for } \langle A_{\text{FB}}^{LL} \rangle, \\ 10^{11} & \text{(for } \langle A_{\text{FB}}^{NN} \rangle, \langle A_{\text{FB}}^{TT} \rangle), \\ 10^{13} & \text{(for } \langle A_{\text{FB}}^{LN} \rangle, \langle A_{\text{FB}}^{NL} \rangle), \\ 10^{11} & \text{(for } \langle A_{\text{FB}}^{LT} \rangle, \langle A_{\text{FB}}^{TL} \rangle), \\ 10^{11} & \text{(for } \langle A_{\text{FB}}^{NT} \rangle, \langle A_{\text{FB}}^{TN} \rangle), \end{cases}$$

(iv) for $\bar{B} \rightarrow \bar{K}^* \tau^+ \tau^-$ decay

$$N \sim \begin{cases} 10^9 & \text{for } \langle A_{\text{FB}} \rangle, \\ 10^9 & \text{for } \langle A_{\text{FB}}^{LL} \rangle, \\ 10^9 & \text{(for } \langle A_{\text{FB}}^{NN} \rangle, \langle A_{\text{FB}}^{TT} \rangle), \\ 10^{12} & \text{(for } \langle A_{\text{FB}}^{LN} \rangle, \langle A_{\text{FB}}^{NL} \rangle), \\ 10^{10} & \text{(for } \langle A_{\text{FB}}^{LT} \rangle, \langle A_{\text{FB}}^{TL} \rangle), \\ 10^{10} & \text{(for } \langle A_{\text{FB}}^{NT} \rangle, \langle A_{\text{FB}}^{TN} \rangle). \end{cases}$$

IV. SUMMARY

To sum up, in this paper by considering the theoretical and experimental uncertainties in the SM we have presented a comprehensive analysis of the polarized and unpolarized forward-backward asymmetries for $\bar{B} \rightarrow \bar{K}_1 \ell^+ \ell^-$ and $\bar{B} \rightarrow \bar{K}^* \ell^+ \ell^-$ decays using model III of 2HDM. At the same time we have compared the results of both decay modes to each other. Also, the minimum required number of events for detecting each asymmetry has been taken into account and compared with the number produced at the LHC experiments, including ATLAS, CMS, and LHCb ($\sim 10^{12}$ per year) or expected to be produced at the Super-LHC experiments (supposed to be $\sim 10^{13}$ per year). In conclusion, the following results have been obtained:

- (i) In the μ channel, no sensitivity has been observed to the nature of produced mesons. Having the vector property or axial-vector property of products does not have any effect on the SM and 2HDM predictions. Since the influences of 2HDM merely on the quantities A_{FB} , A^{LL} , and A^{LT} could be large and the minimum required number of $B\bar{B}$ pairs for the measurement of those asymmetries at the LHC is smaller than 10^{12} , experimental studies of all mentioned asymmetries can be suitable for searching in model III of 2HDM.

- (ii) In the τ channel, while the vector property or the axial-vector property of products could have some effects on the SM and 2HDM predictions, there is the probability that these characteristics do not impose any influence on the deviations from the SM predictions. For instance, the predictions of A^{LL} , A^{LT} , and A^{NT} for all cases and the predictions of A_{FB} for cases B and C, as well as the predictions of A^{NN} for cases A and C, are invariant under the exchange of the axial-vector meson to the vector meson and vice versa. In contrast, the predictions of A^{LN} for all cases and the predictions of A_{FB} only for case A, as well as the predictions of A^{NN} only for case B, are different under the transformation of the axial-vector meson to the vector meson and vice versa. On the other hand, except for the anticipations of A^{LN} for the $\bar{B} \rightarrow \bar{K}_1$ transition and the predictions of A^{LT} for both transitions $\bar{B} \rightarrow \bar{K}_1$ and $\bar{B} \rightarrow \bar{K}^*$, which are completely in the SM intervals, the upper limit, the lower limit, or both of them in the other asymmetries are not in the range of the SM predictions. Also, according to the calculated minimum required number of $B\bar{B}$ pairs for detecting each asymmetry at the LHC, all asymmetries of both transitions except A^{LN} for the $\bar{B} \rightarrow \bar{K}_1$ transition are measurable at the LHC. The A^{LN} asymmetry of $\bar{B} \rightarrow \bar{K}_1 \tau^+ \tau^-$ is detectable at the SLHC. Therefore, based on the above discussion, experimental studies of all of these asymmetries except A^{LN} for $\bar{B} \rightarrow \bar{K}_1$ and A^{LT} for $\bar{B} \rightarrow \bar{K}_1$ and $\bar{B} \rightarrow \bar{K}^*$ can be invaluable for exploring model III of 2HDM.

Finally, it is worthwhile to mention that although the muon polarization is measured for stationary muons, such experiments are very hard to perform in the near future. The tau polarization can be studied by investigating the decay products of tau. The measurement of tau polarization in this respect is easier than the polarization of the muon.

ACKNOWLEDGMENTS

The authors would like to thank V. Bashiry for his useful discussions. The support of the Research Council of Shiraz University is gratefully acknowledged.

APPENDIX

The auxiliary functions $\mathcal{A}^{K_1}(\hat{s})$, \dots , $\mathcal{H}^{K_1}(\hat{s})$ are defined as

$$\mathcal{A}^{K_1}(\hat{s}) = \frac{2}{1 + \sqrt{\hat{r}_{K_1}}} c_9^{\text{eff}}(\hat{s}) A^{K_1}(\hat{s}) + \frac{4(\hat{m}_b - \hat{m}_s)}{\hat{s}} c_7^{\text{eff}} T_1^{K_1}(\hat{s}), \quad (\text{A1})$$

$$\mathcal{B}^{K_1}(\hat{s}) = \left(1 + \sqrt{\hat{r}_{K_1}}\right) \left[c_9^{\text{eff}}(\hat{s}) V_1^{K_1}(\hat{s}) + \frac{2(\hat{m}_b + \hat{m}_s)}{\hat{s}} \left(1 - \sqrt{\hat{r}_{K_1}}\right) c_7^{\text{eff}} T_2^{K_1}(\hat{s}) \right], \quad (\text{A2})$$

$$\mathcal{C}^{K_1}(\hat{s}) = \frac{1}{1 - \hat{r}_{K_1}} \left[\left(1 - \sqrt{\hat{r}_{K_1}}\right) c_9^{\text{eff}}(\hat{s}) V_2^{K_1}(\hat{s}) + 2(\hat{m}_b + \hat{m}_s) c_7^{\text{eff}} \left(T_3^{K_1}(\hat{s}) + \frac{1 - \hat{r}_{K_1}}{\hat{s}} T_2^{K_1}(\hat{s}) \right) \right], \quad (\text{A3})$$

$$\mathcal{D}^{K_1}(\hat{s}) = \frac{1}{\hat{s}} \left[c_9^{\text{eff}}(\hat{s}) \left\{ \left(1 + \sqrt{\hat{r}_{K_1}}\right) V_1^{K_1}(\hat{s}) - \left(1 - \sqrt{\hat{r}_{K_1}}\right) V_2^{K_1}(\hat{s}) - 2\sqrt{\hat{r}_{K_1}} V_0^{K_1}(\hat{s}) \right\} - 2(\hat{m}_b + \hat{m}_s) c_7^{\text{eff}} T_3^{K_1}(\hat{s}) \right], \quad (\text{A4})$$

$$\mathcal{E}^{K_1}(\hat{s}) = \frac{2}{1 + \sqrt{\hat{r}_{K_1}}} c_{10} A^{K_1}(\hat{s}), \quad (\text{A5})$$

$$\mathcal{F}^{K_1}(\hat{s}) = \left(1 + \sqrt{\hat{r}_{K_1}}\right) c_{10} V_1^{K_1}(\hat{s}), \quad (\text{A6})$$

$$\mathcal{G}^{K_1}(\hat{s}) = \frac{1}{1 + \sqrt{\hat{r}_{K_1}}} c_{10} V_2^{K_1}(\hat{s}), \quad (\text{A7})$$

$$\mathcal{H}^{K_1}(\hat{s}) = \frac{1}{\hat{s}} c_{10} \left[\left(1 + \sqrt{\hat{r}_{K_1}}\right) V_1^{K_1}(\hat{s}) - \left(1 - \sqrt{\hat{r}_{K_1}}\right) V_2^{K_1}(\hat{s}) - 2\sqrt{\hat{r}_{K_1}} V_0^{K_1}(\hat{s}) \right], \quad (\text{A8})$$

$$\mathcal{I}_1^{K_1}(\hat{s}) = -\frac{(1 + \hat{m}_s)}{\hat{m}_b + \hat{m}_s} \left[C_{Q_1} \left(1 + \sqrt{\hat{r}_{K_1}}\right) V_1^{K_1}(\hat{s}) \right], \quad (\text{A9})$$

$$\mathcal{J}_1^{K_1}(\hat{s}) = \frac{(1 + \hat{m}_s)}{\hat{m}_b + \hat{m}_s} \left[C_{Q_1} \left\{ -\left(1 - \sqrt{\hat{r}_{K_1}}\right) V_2^{K_1}(\hat{s}) + 2\sqrt{\hat{r}_{K_1}} [V_3^{K_1}(\hat{s}) - V_0^{K_1}(\hat{s})] \right\} \right], \quad (\text{A10})$$

$$\mathcal{I}_2^{K_1}(\hat{s}) = \mathcal{I}_1^{K_1}(\hat{s})(C_{Q_1} \rightarrow C_{Q_2}), \quad \mathcal{J}_2^{K_1}(\hat{s}) = \mathcal{J}_1^{K_1}(\hat{s})(C_{Q_1} \rightarrow C_{Q_2}), \quad (\text{A11})$$

with $\hat{r}_{K_1} = m_{K_1}^2/m_B^2$. The $\Delta(\hat{s})$ function is obtained as

$$\begin{aligned} \Delta(\hat{s}) = & \frac{8\text{Re}[\mathcal{F}\mathcal{H}^*]\hat{m}_\ell^2\lambda}{\hat{r}_{K_1}} + \frac{8\text{Re}[\mathcal{G}\mathcal{H}^*]\hat{m}_\ell^2(-1 + \hat{r}_{K_1})\lambda}{\hat{r}_{K_1}} - \frac{4|\mathcal{H}|^2\hat{m}_\ell^2\hat{s}\lambda}{\hat{r}_{K_1}} - \frac{|\mathcal{C}|^2\lambda(3 + 3\hat{r}_{K_1}^2 - 6\hat{s} + 3\hat{s}^2 - 6\hat{r}_{K_1}(1 + \hat{s}) - v^2\lambda)}{3\hat{r}_{K_1}} \\ & - \frac{|\mathcal{G}|^2\lambda(3 + 3\hat{r}_{K_1}^2 + 12\hat{m}_\ell^2(2 + 2\hat{r}_{K_1} - \hat{s}) - 6\hat{s} + 3\hat{s}^2 - 6\hat{r}_{K_1}(1 + \hat{s}) - v^2\lambda)}{3\hat{r}_{K_1}} \\ & + \frac{|\mathcal{F}|^2(-3 - 3\hat{r}_{K_1}^2 + 6\hat{r}_{K_1}(1 + 16\hat{m}_\ell^2 - 3\hat{s}) + 6\hat{s} - 3\hat{s}^2 + v^2\lambda)}{3\hat{r}_{K_1}} \\ & + \frac{|\mathcal{B}|^2(-3 - 3\hat{r}_{K_1}^2 + 6\hat{r}_{K_1}(1 - 8\hat{m}_\ell^2 - 3\hat{s}) + 6\hat{s} - 3\hat{s}^2 + v^2\lambda)}{3\hat{r}_{K_1}} \\ & - \frac{4}{3} |\mathcal{A}|^2(2\hat{m}_\ell^2 + \hat{s})\lambda + |\mathcal{E}|^2 \left(4\hat{m}_\ell^2\lambda - \frac{\hat{s}}{3} (3 + 3\hat{r}_{K_1}^2 - 6\hat{s} + 3\hat{s}^2 - 6\hat{r}_{K_1}(1 + \hat{s}) + v^2\lambda) \right) \\ & + \lambda \left\{ \frac{(4\hat{m}_\ell^2 - \hat{s})|\mathcal{I}_1|^2}{\hat{r}_{K_1}} + \frac{|\mathcal{J}_1|^2(4\hat{m}_\ell^2 - \hat{s})}{\hat{r}_{K_1}} + \frac{2\text{Re}[\mathcal{I}_1\mathcal{J}_1^*](4\hat{m}_\ell^2 - \hat{s})}{\hat{r}_{K_1}} - \frac{|\mathcal{I}_2|^2\hat{s}}{\hat{r}_{K_1}} - \frac{|\mathcal{J}_2|^2\hat{s}}{\hat{r}_{K_1}} - \frac{2\text{Re}[\mathcal{I}_2\mathcal{J}_2^*]\hat{s}}{\hat{r}_{K_1}} + \frac{4\text{Re}[\mathcal{H}\mathcal{I}_2^*]\hat{m}_\ell\hat{s}}{\hat{r}_{K_1}} \right. \\ & \left. + \frac{4\text{Re}[\mathcal{H}\mathcal{J}_2^*]\hat{m}_\ell\hat{s}}{\hat{r}_{K_1}} - \frac{4\text{Re}[\mathcal{F}\mathcal{I}_2^*]\hat{m}_\ell\hat{s}}{\hat{r}_{K_1}} - \frac{4\text{Re}[\mathcal{F}\mathcal{J}_2^*]\hat{m}_\ell\hat{s}}{\hat{r}_{K_1}} - \frac{4\text{Re}[\mathcal{G}\mathcal{I}_2^*]\hat{m}_\ell(\hat{r}_{K_1} - 1)}{\hat{r}_{K_1}} - \frac{4\text{Re}[\mathcal{G}\mathcal{J}_2^*]\hat{m}_\ell(\hat{r}_{K_1} - 1)}{\hat{r}_{K_1}} \right\} \\ & - \frac{2\text{Re}[\mathcal{B}\mathcal{C}^*](-1 + \hat{r}_{K_1} + \hat{s})(3 + 3\hat{r}_{K_1}^2 - 6\hat{s} + 3\hat{s}^2 - 6\hat{r}_{K_1}(1 + \hat{s}) - v^2\lambda)}{3\hat{r}_{K_1}} \\ & + \frac{2\text{Re}[\mathcal{F}\mathcal{G}^*](12\hat{m}_\ell^2\lambda - (-1 + \hat{r}_{K_1} + \hat{s})(3 + 3\hat{r}_{K_1}^2 - 6\hat{s} + 3\hat{s}^2 - 6\hat{r}_{K_1}(1 + \hat{s}) - v^2\lambda))}{3\hat{r}_{K_1}}. \end{aligned} \quad (\text{A12})$$

- [1] H. Hatanaka and K. C. Yang, *Phys. Rev. D* **78**, 074007 (2008).
- [2] R. H. Li, C. D. Lu, and W. Wang, *Phys. Rev. D* **79**, 094024 (2009).
- [3] M. A. Paracha, I. Ahmed, and M. J. Aslam, *Eur. Phys. J. C* **52**, 967 (2007).
- [4] V. Bashiry, *J. High Energy Phys.* 06 (2009) 062.
- [5] I. Ahmed, M. A. Paracha, and M. J. Aslam, *Eur. Phys. J. C* **54**, 591 (2008); A. Saddique, M. J. Aslam, and C. D. Lu, *Eur. Phys. J. C* **56**, 267 (2008); I. Ahmed, M. A. Paracha, and M. J. Aslam, *Eur. Phys. J. C* **71**, 1521 (2011).
- [6] V. Bashiry and K. Azizi, *J. High Energy Phys.* 01 (2010) 033.
- [7] A. Ahmed, I. Ahmed, M. A. Paracha, and A. Rehman, *Phys. Rev. D* **84**, 033010 (2011).
- [8] Y. Li, J. Hua, and K. C. Yang, *Eur. Phys. J. C* **71**, 1775 (2011).
- [9] C. Csaki, *Mod. Phys. Lett. A* **11**, 599 (1996).
- [10] D. Atwood, L. Reina, and A. Soni, *Phys. Rev. D* **55**, 3156 (1997).
- [11] S. Glashow and S. Weinberg, *Phys. Rev. D* **15**, 1958 (1977).
- [12] D. Bowser-Chao, K. Cheung, and W. Y. Keung, *Phys. Rev. D* **59**, 115006 (1999).
- [13] B. Grinstein, M. J. Savage, and M. B. Wise, *Nucl. Phys.* **B319**, 271 (1989).
- [14] A. J. Buras and M. Munz, *Phys. Rev. D* **52**, 186 (1995).
- [15] Y. B. Dai, C. S. Huang, and H. W. Huang, *Phys. Lett. B* **390**, 257 (1997).
- [16] F. Kruger and L. M. Sehgal, *Phys. Lett. B* **380**, 199 (1996).
- [17] P. Ball and V. M. Braun, *Phys. Rev. D* **58**, 094016 (1998).
- [18] K. C. Yang, *Phys. Rev. D* **78**, 034018 (2008).
- [19] C. S. Huang and S. H. Zhu, *Phys. Rev. D* **68**, 114020 (2003).
- [20] Y. B. Dai, C. S. Huang, J. T. Li, and W. J. Li, *Phys. Rev. D* **67**, 096007 (2003).
- [21] M. Suzuki, *Phys. Rev. D* **47**, 1252 (1993).
- [22] L. Burakovsky and T. Goldman, *Phys. Rev. D* **57**, 2879 (1998).
- [23] H. Y. Cheng, *Phys. Rev. D* **67**, 094007 (2003).
- [24] H. Hatanaka and K. C. Yang, *Phys. Rev. D* **77**, 094023 (2008).
- [25] G. Abbiendi *et al.* (OPAL Collaboration), *Phys. Lett. B* **492**, 23 (2000).
- [26] A. Rouge, *Z. Phys. C* **48**, 75 (1990); in *Proceedings of the Workshop on τ Lepton Physics, Orsay, France, 1990*.